CALIFORNIA INSTITUTE OF TECHNOLOGY

EARTHQUAKE ENGINEERING RESEARCH LABORATORY

ON THE SOLUTION OF FIRST-EXCURSION FAILURE PROBLEM FOR LINEAR SYSTEMS BY EFFICIENT SIMULATION

BY

S. K. AU AND J. L. BECK

REPORT NO. EERL 2000-01

A REPORT ON RESEARCH PARTIALLY SUPPORTED BY
THE PACIFIC EARTHQUAKE ENGINEERING RESEARCH CENTER UNDER A
NATIONAL SCIENCE FOUNDATION COOPERATIVE AGREEMENT
PASADENA, CALIFORNIA

NOVEMBER 2000

A REPORT ON RESEARCH PARTIALLY SUPPORTED BY THE PACIFIC EARTHQUAKE ENGINEERING RESEARCH CENTER UNDER NATIONAL SCIENCE FOUNDATION COOPERATIVE AGREEMENT NO. CMS-9701568

On the Solution of First-Excursion Failure Problem for Linear Systems by Efficient Simulation

S. K. Au and J. L. Beck
Division of Engineering and Applied Science,
California Institute of Technology,
Pasadena, CA 91125

Oct 2000

Abstract

An analytical study of the failure region of the first-excursion reliability problem for linear dynamical systems subjected to Gaussian white noise excitation is carried out with a view to constructing a suitable importance sampling density for computing the first-excursion failure probability. Central to the study are 'elementary failure regions', which are defined as the failure region in the load space corresponding to the failure of a particular output response at a particular instant. Each elementary failure region is completely characterized by its design point, which can be computed readily using impulse response functions of the system. It is noted that the complexity of the first-excursion problem stems from the structure of the union of the elementary failure regions. One important consequence of this union structure is that, in addition to the global design point, a large number of neighboring design points are important in accounting for the failure probability. Using information from the analytical study, an importance sampling density is proposed. Numerical examples are presented, which demonstrate that the efficiency of using the proposed importance sampling density to calculate system reliability is remarkable.

Contents

1 Introduction **1**

2 Discrete-time linear systems **5**

3 Analysis of the failure region **7**

3.1 Elementary failure region 7

3.2 Interaction of elementary failure regions 10

4 Development of importance sampling density **14**

4.1 Proposed ISD 16

4.2 Simulation of samples according to the proposed ISD 17

4.3 Properties of proposed ISD and failure probability estimator 18

5 Summary of proposed importance sampling procedure **21**

6 Numerical applications **23**

6.1 Example 1: SDOF oscillator 23

6.2 Example 2: Seismic response of moment-resisting steel frame 26

7 Conclusions **35**

A Some additional observations on the failure region of SDOF time-invariant linear systems **36**

A.1 Neighborhood of points in the failure region 36

A.2 Proximity of neighboring design points 37

A.3 Overshooting of design point response 39

A.4 A reciprocal relationship of design point responses 41

B Simulation formula for $\boldsymbol{Z}_i^{\perp}$ **42**

List of Tables

1 The c.o.v. Δ of importance sampling quotients for failure probability . . . 26
2 Number of samples N_δ to achieve a c.o.v. of $\delta = 30\%$ in $\tilde{P}_F$ 27
3 Sections (AISC) for frame members 28
4 Point Masses 28
5 The c.o.v. Δ of proposed importance sampling quotient for failure probability for peak interstory drift ratio 31
6 Failure probability estimates for peak interstory drift ratio with $N = 20$ samples 31
7 The c.o.v. Δ of proposed importance sampling quotient for failure probability for peak floor acceleration 33
8 Failure probability estimates for peak floor acceleration with $N = 20$ samples 33

List of Figures

1 Neighboring design points 11

2 Variation with time of reliability index β_k, response standard deviation σ_k and impulse response $g(k)$ 12

3 Impulse response function $h(t)$ 23

4 Standard deviation of response, $\sigma(t)$ 24

5 Weight $w(t)$ 24

6 Failure probability estimates for different threshold levels b and number of samples N. Choice (1): dotted lines; Choice (2): dashed lines; Choice (3): solid lines; MCS with 10^6 samples: asterisks 25

7 Moment-resisting frame structure 27

8 Impulse response $h_i(t)$, standard deviation $\sigma_i(t)$ and elementary failure probability $P_i(t)$ for interstory drift ratios 30

9 Failure probability estimates for peak interstory drift ratio for different threshold levels b and number of samples N. MCS estimates with $10,000$ samples are shown with circles 32

10 Impulse response $h_i(t)$, standard deviation $\sigma_i(t)$ and elementary failure probability $P_i(t)$ for floor accelerations 34

11 Failure probability estimates for peak floor acceleration for different threshold levels b and number of samples N. MCS estimates with $10,000$ samples are shown with circles 34

1 Introduction

In the reliability analysis of dynamical systems subjected to uncertain excitation modeled by stochastic processes, an important problem is to determine the first-excursion probability that any one of m output states of interest, $Y_i(t)$, $i = 1, \ldots, m$, exceeds in magnitude some specified threshold level $b_i(t)$ within a given time duration T:

$$P_F = P(F) = P(\bigcup_{i=1}^{m} \{\exists t \in [0,T] : |Y_i(t)| > b_i(t)\}) \tag{1}$$

where F denotes the 'failure' event of interest. This problem is commonly known as the first-excursion (or first passage) problem, which is among the most difficult problems in the theory of stochastic dynamics. In spite of the enormous amount of attention the problem has received, there is no procedure available for its *general* solution, especially for engineering problems of interest where the number of output states m is large and the failure probability P_F is small.

Pioneered by Rice, early work on the first-excursion problem was focused on out-crossing theory to give an analytical approximation (Rice 1944; Rice 1945; Crandall et al. *1966; Yang and Shinozuka 1971; Vanmarcke 1975; Mason and Iwan 1983; Langley 1988;* Naess 1990). While the analytical solutions from out-crossing theory offer important insights into the problem, they are nevertheless approximate and applicable only for a single output state (i.e., $m = 1$). A class of numerical solution methods involves solving the backward Kolmogorov equation for the reliability function (Roberts 1976; Bergman and Heinrich 1981; Spencer and Bergman 1993). These numerical solutions are limited in application to systems of small size since their complexity increases at least exponentially with the state-space dimension of the system (Lin and Cai 1995; Schuëller et al. 1993).

Simulation methods offer a feasible alternative for the numerical solution of first-excursion problems with larger state-space dimensions. In this approach, the stochastic excitation is specified by a finite number of 'input random variables', $Z_1, \ldots, Z_n$, which can be simulated to generate a realization of the excitation (*Shinozuka 1987; Shinozuka and* Deodatis 1988). In terms of the joint probability density function (PDF) p for the input random variables, the failure probability can be written as a classical probability integral:

$$P_F = \int_F p(\boldsymbol{z})d\boldsymbol{z} = \int \mathbb{I}_F(\boldsymbol{z})p(\boldsymbol{z})d\boldsymbol{z} = \mathsf{E}[\mathbb{I}_F(\boldsymbol{Z})] \tag{2}$$

where $\boldsymbol{z} = [z_1, \ldots, z_n]$ is a state of the input random variables which generate the excitation, and $\mathbb{I}_F(\cdot)$ is the indicator function: $\mathbb{I}_F(\boldsymbol{z}) = 1$ if $\boldsymbol{z} \in F$ and $\mathbb{I}_F(\boldsymbol{z}) = 0$ otherwise. Here, F is interpreted as the failure region in the n-dimensional space of $\boldsymbol{z}$. The last expression in (2) views P_F as the expectation of the indicator function $\mathbb{I}_F(\boldsymbol{Z})$ when $\boldsymbol{Z} = [Z_1, \ldots, Z_n]$ is distributed according to p. This perspective is the basis for Monte Carlo simulation (Rubinstein 1981; Hammersley and Handscomb 1964), where P_F is estimated as the average of the indicator function $\mathbb{I}_F(\boldsymbol{Z}_r)$ among the independent and identically distributed (i.i.d.) samples $\{\boldsymbol{Z}_r : r = 1, \ldots, N\}$ simulated according to p. As is well known, Monte Carlo simulation is not computationally efficient for estimating small P_F, since the number of samples required to achieve a given accuracy is inversely proportional to P_F when P_F is small. Essentially, estimating small probabilities requires information from rare samples which lead to failure, and on average it requires many samples before one such failure sample occurs. In view of this, the importance sampling method (Rubinstein 1981; Schuëller and Stix 1987) has been introduced to compute P_F, which basically shifts the sampling density towards the failure region F so as to produce more samples lying in F. The efficiency of the method relies on a proper choice of the importance sampling density (ISD), which inevitably requires some knowledge about the failure region.

For time-invariant or static problems, many schemes for constructing the ISD, such as those based on design point(s) (Schuëller and Stix 1987; Melchers 1989; Papadimitriou et al. 1997; Der Kiureghian and Dakessian 1998; Au et al. 1999) or pre-samples (Bucher 1988; Karamchandani et al. 1989; Ang et al. 1992; Au and Beck 1999) are found to be useful. The design point(s) or pre-samples are often obtained numerically by optimization or simulation where the integrand function $\mathbb{I}_F(\boldsymbol{z})p(\boldsymbol{z})$ is directly used. In those cases where the dimension of the uncertain parameter space is not too large and the failure region is relatively simple to describe, the information from the design point(s) or pre-samples is sufficient to characterize the failure region, and hence yields a good importance sampling density. For time-varying reliability problems such as the first-excursion problem, the dimension of the uncertain parameter space is often very large, paralleled by a dramatic increase in complexity of the failure region. The construction of the ISD using information numerically extracted from the integrand function $\mathbb{I}_F(\boldsymbol{z})p(\boldsymbol{z})$ becomes much more difficult. Some attempts have been presented to adapt the ISD using spectral information from some pre-samples of the response (Bayer and Bucher 1999), but reported applications have been limited to cases when the number of spectral components (and hence the number of uncertain parameters)

in the discrete spectral representation of the excitation is not large (e.g., less than 100) which inevitably imposes restrictions on the approximate representation of the excitation in practical applications.

In view of the aforementioned difficulties in applying existing simulation techniques to solve the first-excursion problem, simulation methods have been developed recently that rely less critically on sampling distributions and that adapt samples in the failure region in a probabilistically correct and reasonably efficient manner. Examples are controlled Monte Carlo simulation (Pradlwarter et al. 1994; Pradlwarter and Schuëller 1997a; Pradlwarter and Schuëller 1997b; Pradlwarter and Schuëller 1999) which is applicable to deterministic systems subjected to uncertain excitations, and subset simulation (Au and Beck 2000a; Au and Beck 2000b) which is applicable to systems with both parametric (e.g., structural) as well as excitation uncertainties. These methods are robust in application and have shown promise to be suitable for general dynamical systems with no restrictions on the type of structural model (linear, nonlinear hysteretic, etc), state-space dimension, number of uncertain parameters in the discrete representation of the excitation, and the probability level. However, one should realize that *the efficiency of a reliability method depends on how much information about a given problem the method has utilized*; additional information can often be exploited to accelerate convergence of the failure probability estimate. In essence, efficiency of a reliability method is often gained at the expense of generality. The aforementioned simulation methods are applicable for general systems and assume no specific structure in the system, suggesting that there may be room for more efficient methods for a certain class of systems by utilizing (if possible) information pertinent to the problem. It is the focus of this work to explore this possibility for an important class of systems – linear dynamical systems.

The random vibration aspects of linear dynamical systems have been studied extensively in the literature (Lin 1967; Soong and Grigoriu 1993; Lin and Cai 1995; Lutes and Sarkani 1997). In particular, for Gaussian excitations, the response at multiple time instants are jointly Gaussian, and their joint probability distribution can be described based on unit impulse response functions. In the context of simulation where a discrete approximation of the excitation is used, the failure region corresponding to the failure of a particular output response at a particular time instant is a half space defined by a hyperplane in the load space. This 'elementary failure region' is completely described by a local design point, which can be obtained from unit impulse response functions. This fact has been

appreciated in a recent work by Der Kiureghian (2000). Recognition of this fact, however, only offers the solution for the failure probability that a *particular* response at a *particular* time exceeds (in magnitude) a given threshold level. The information that is still missing for evaluating the first-excursion probability, which is the probability that *any* one of the output response of interest exceeds (in magnitude) the given threshold level at *any* time instant within the duration of study, is rooted in the interaction of the elementary failure regions corresponding to each of the output responses at each time instant within the time duration of interest.

In this work, we focus on constructing an efficient ISD for evaluating the first-excursion probability for linear systems under Gaussian white-noise excitation. For this purpose, we investigate the failure region from the perspective of viewing the failure event as a union of elementary failure events. Based on information from this study, we propose an ISD which is shown to be very efficient compared to conventional ISDs constructed using information numerically obtained from the integrand function. Numerical applications are presented to demonstrate the superior efficiency of the proposed ISD, showing that the analytical investigation of the failure region is highly rewarding.

2 Discrete-time linear systems

We first describe the linear systems considered in the first-excursion problem. By linear systems we mean that the relationship between the input excitation and the output response quantity of interest is linear. For convenience in notation, we will use braced quantities to denote the set of quantities inside the brace generated by running the subscripted index or indexes of the brace over their whole range. For example, $\{Z_i\}_i = \{Z_1, \ldots, Z_n\}$ where it is understood that there are n random variables in the specification of the excitation.

Let $W_1(t), \ldots, W_l(t)$ and $Y_1(t), \ldots, Y_m(t)$ be respectively the l input (excitation) and m output (response) time histories of a continuous-time linear system. Without loss of generality, the outputs are assumed to start from zero initial conditions at time $t = 0$. The input-output relationship can be generally written as, for $i = 1, \ldots, m$,

$$Y_i(t) = \sum_{j=1}^{l} \int_0^t h_{ij}(t, \tau) W_j(\tau) d\tau \tag{3}$$

where $h_{ij}(t, \tau)$ is the unit impulse response function (or Green's function) for the i-th output at time t due to a unit impulse applied at the j-th input at time τ. As a result of linearity, the response is a sum of the contributions from the individual input W_j. Causality has been assumed for the impulse response functions, namely, $h_{ij}(t, \tau) \equiv 0$ for $t < \tau$, so that the integration limit is from 0 to t instead of 0 to ∞. The representation in (3) is applicable for any linear system, including time-varying systems.

In practical applications, the output response is often solved at discrete time steps by some numerical integration scheme (Dokainish and Subbaraj 1989; Subbaraj and Dokainish 1989) using the values of the input at the sampled time instants. Let the sampling be uniform at time spacing $\Delta t = T/(n_t - 1)$ where T is the duration of study and n_t is the number of time points, so that the sampling times are $t_k = (k-1)\Delta t$, $k = 1, \ldots, n_t$. The excitation $\{W_j\}_j$ in discrete-time is assumed to be band-limited Gaussian white noise:

$$W_j(t_k) = \sqrt{\frac{2\pi S_j}{\Delta t}} Z_j(k) \tag{4}$$

where S_j is the spectral intensity and $\{Z_j(k)\}_{jk}$ are i.i.d. Gaussian random variables. In the discrete-time system, $\{Z_j(k)\}_{jk}$ are considered as the input random variables, from which a realization of the excitation can be generated for simulation purposes. The vector $\boldsymbol{Z} = [Z_1(1), \ldots, Z_l(1), \ldots, Z_1(n_t), \ldots, Z_l(n_t)]$ collecting all the input random variables is

thus an $n = n_t \times l$-dimensional standard Gaussian vector with independent components and so has joint PDF

$$p(\boldsymbol{z}) = \phi(\boldsymbol{z}) \triangleq (2\pi)^{-n/2} \exp(-\frac{1}{2}\sum_{i=1}^{n} z_i^2) \tag{5}$$

where $\boldsymbol{z} = [z_1, \ldots, z_n]$ is a state of the input random vector $\boldsymbol{Z}$. Although the excitation is assumed to be stationary white noise in (4), the formulation is applicable for more general excitation by redefining the system. For example, if the excitation is a filtered white noise modulated by an envelope function, then h_{ij} will be equal to the convolution of the impulse response function of the original system and the filter, multiplied by the envelope function.

Using the representation of the excitation in (4), the discrete-time analog of the input-output relationship in (3) can be written in terms of the input random variables $\{Z_j(s)\}_{js}$:

$$Y_i(k) = \sum_{j=1}^{l}\sum_{s=1}^{k} g_{ij}(k,s) Z_j(s) \sqrt{2\pi S_j \Delta t} \tag{6}$$

where $\{Y_i(k)\}_i$ are the outputs at time step k and $g_{ij}(k,s)$ is the discrete-time unit impulse response of the i-th output at time step k due to a unit impulse $Z_j(s) = 1$ applied at the j-th input at time step s. The relationship between g_{ij} and h_{ij} depends on the numerical integration scheme used. The discrete-time impulse response g_{ij} can often be obtained numerically from dynamic analysis using finite element programs, for example. In particular, for time-invariant systems, $h_{ij}(t,\tau) = h_{ij}(t-\tau)$ and $g_{ij}(k,s) = g_{ij}(k-s+1)$, so the set of impulse response functions $\{g_{ij}(k,s)\}_i$ corresponding to the j-th input excitation can be obtained in one dynamic analysis. Consequently, it requires l dynamic analyses to obtain the whole set of impulse response functions $\{g_{ij}\}_{ij}$ which completely describe the input-output relationship.

As a fact that will be used later, it is noted that the discrete impulse response will tend to its continuous-time counterpart as the sampling interval Δt tends to zero:

$$g_{ij}(k,s) \to h_{ij}(t_k, t_s) \quad \text{as } \Delta t \to 0 \tag{7}$$

provided that the numerical scheme used to compute the response is convergent (i.e., consistent and stable) (Hughes 1987). In practical applications where the numerical scheme is sufficiently accurate, it may be assumed that the discrete-time and continuous-time impulse responses are equal at the sampled time instants.

3 Analysis of the failure region

In terms of the discrete-time system, the failure event F of interest is defined as the exceedence of the absolute response of any one of the outputs beyond a given threshold level at any time step between 1 and n_t:

$$F = \bigcup_{i=1}^{m} \bigcup_{k=1}^{n_t} \{|Y_i(k)| > b_i(k)\} = \bigcup_{i=1}^{m} \bigcup_{k=1}^{n_t} F_{ik} \tag{8}$$

where $b_i(k)$ is the threshold level for the i-th output at time step k, and F_{ik} is the 'elementary failure event' that the absolute response of the i-th output at time step k exceeds $b_i(k)$, that is,

$$F_{ik} = \{|Y_i(k)| > b_i(k)\} \tag{9}$$

Since F is the union of the elementary failure events $\{F_{ik}\}_{ik}$, a study of the latter may help understand the former. We will thus begin by studying the elementary failure event F_{ik} for given i and k.

3.1 Elementary failure region

The elementary failure event F_{ik} is the union of the up-crossing and down-crossing events, $F_{ik}^+ = \{Y_i(k) > b_i(k)\}$ and $F_{ik}^- = \{Y_i(k) < -b_i(k)\}$, respectively, which are mutually exclusive. Since F_{ik}^- can be written as $\{-Y_i(k) > b_i(k)\}$, that is, the up-crossing event of $-Y_i$ at time step k, and the two processes Y_i and $-Y_i$ are probabilistically identical, it suffices to consider the up-crossing event F_{ik}^+. Using (6), F_{ik}^+ is the semi-infinite region $\{\boldsymbol{z} : \sum_{j=1}^{l} \sum_{s=1}^{k} g_{ij}(k,s) z_j(s) \sqrt{2\pi S_j \Delta t} > b_i(k)\}$ in the standard n-dimensional Gaussian space of the input variables $\boldsymbol{z}$. The failure boundary is given by $\partial F_{ik}^+ = \{\boldsymbol{z} : \sum_{j=1}^{n} \sum_{s=1}^{k} g_{ij}(k,s) z_j(s) \sqrt{2\pi S_j \Delta t} = b_i(k)\}$, which is a hyperplane in the n-dimensional space of $\boldsymbol{z}$. Note that ∂F_{ik}^+ imposes a constraint only on $\boldsymbol{z}_j(s)$ for all $s \leq k$, as a result of *causality*.

Design point

The point in F_{ik}^+ which has the highest probability density among other points in F_{ik}^+, called the design point for F_{ik}^+ in reliability terminology, is of particular importance. As the PDF $\phi(\boldsymbol{z})$ for $\boldsymbol{Z}$ decays radially from the origin, the design point lies on the failure boundary ∂F_{ik}^+. The design point maximizes the joint PDF $\phi(\boldsymbol{z})$ under the linear constraint

$\sum_{j=1}^{l}\sum_{s=1}^{k} g_{ij}(k,s)z_j(s)\sqrt{2\pi S_j\Delta t} = b_i(k)$. Since $\phi(\boldsymbol{z})$ is a decreasing function of only the distance of $\boldsymbol{z}$ from the origin, which is equal to the Euclidean norm of $\boldsymbol{z}$, the design point is just the point on ∂F_{ik}^{+} with the smallest Euclidean norm. Let $\boldsymbol{z}_{ik}^{*} = \{z_{ik,j}^{*}(s)\}_{js} \in \mathbb{R}^n$ be the design point of the elementary failure event F_{ik}^{+}, where $z_{ik,j}^{*}(s)$ is the value of the j-th input at time step s corresponding to the design point. Direct constraint minimization yields:

$$z_{ik,j}^{*}(s) = U(k-s)\sqrt{2\pi S_j\Delta t}\,\frac{g_{ij}(k,s)}{\sigma_{ik}^2}b_i(k) \tag{10}$$

where $U(\cdot)$ is the unit step function: $U(x) = 1$ if $x \geq 0$ and zero otherwise, and

$$\sigma_{ik}^2 = \mathsf{Var}[Y_i(k)] = \sum_{j=1}^{m}[\sum_{s=1}^{k} g_{ij}(k,s)^2]2\pi S_j\Delta t \tag{11}$$

is the variance of $Y_i(k)$, which can be readily obtained by direct analysis of (6). As a consequence of causality, $z_{ik,j}^{*}(s) = 0$ for $s > k$. It is interesting to note that the variance σ_{ik}^2 of the i-th output at time step k is equal to the sum of all the 'energy' of the corresponding impulse responses from all inputs accumulated up to time step k. By (7), $g_{ij}(k,s) \to h_{ij}(t_k,t_s)$ as $\Delta t \to 0$, so we have

$$\begin{aligned}\sigma_{ik}^2 &\to \sum_{j=1}^{m} 2\pi S_j \int_0^{t_k} h_{ij}(t_k,\tau)^2 d\tau \quad \text{as } \Delta t \to 0 \\ &= \text{variance of output } i \text{ at time } t_k \text{ of continuous-time system}\end{aligned} \tag{12}$$

and so σ_{ik}^2 varies 'continuously' with k as the sampling is refined.

The excitation $W_{ik,j}^{*}$ at the j-th input that corresponds to the design point $\boldsymbol{z}_{ik,j}^{*}$ is

$$W_{ik,j}^{*}(t_s) = \sqrt{\frac{2\pi S_j}{\Delta t}}\boldsymbol{z}_{ik,j}^{*}(s) = U(k-s)\frac{g_{ij}(k,s)}{\sum_{j=1}^{m}\sum_{s=1}^{k} g_{ij}(j,s)^2\Delta t}b_i(k) \tag{13}$$

and so

$$W_{ik,j}^{*}(t_s) \to\ U(t_k-t_s)b_i(k)\frac{h_{ij}(t_k,t_s)}{\int_0^t h_{ij}(t_k,\tau)^2 d\tau} \quad \text{as } \Delta t \to 0 \tag{14}$$

Reliability index and probability content

The Euclidean norm β_{ik} of the design point $\boldsymbol{z}_{ik}^{*}$, often called the 'reliability index', is given by:

$$\beta_{ik} = ||z_{ik}^{*}|| = \frac{b_i(k)}{\sigma_{ik}} \tag{15}$$

Since the components of $\boldsymbol{z}$ are i.i.d. standard Gaussian, the probability content of F_{ik}^{+} is given by

$$P(F_{ik}^{+}) = \Phi(-||z_{ik}^{*}||) = \Phi(-\beta_{ik}) \tag{16}$$

where $\Phi(\cdot)$ is the cumulative distribution function of the standard Gaussian distribution. Equation (16) can be obtained directly by noting that the i-th output has Gaussian distribution with mean zero and standard deviation σ_{ik} for a linear system under zero mean Gaussian excitation. Note that in the present case where the failure boundary is a hyperplane, the probability content of the failure region F_{ik}^{+} is completely determined by the reliability index β_{ik}.

Conditional distribution of input random variables

The conditional distribution of the input random vector $\boldsymbol{Z}$ given that it lies in the elementary failure region F_{ik}^{+} is just the original PDF $\phi(\boldsymbol{z})$ confined to F_{ik}^{+} and normalized by the probability content of F_{ik}^{+}:

$$p(\boldsymbol{z}|F_{ik}^{+}) = \frac{\phi(\boldsymbol{z})\mathbb{I}_{F_{ik}^{+}}(\boldsymbol{z})}{\Phi(-\beta_{ik})} \tag{17}$$

The simulation formula for a random vector distributed according to $p(\boldsymbol{z}|F_{ik}^{+})$ in (17) can be derived by imposing the conditioning F_{ik}^{+} on the unconditional vector $\boldsymbol{Z}$ which has standard Gaussian distribution with independent components. Let $\{\boldsymbol{v}_1, \ldots, \boldsymbol{v}_n\}$ be any orthonormal basis in $\mathbb{R}^n$. By the rotational symmetry of a standard Gaussian vector with independent components, $\boldsymbol{Z}$ can be represented as

$$\boldsymbol{Z} = \sum_{j=1}^{n} \xi_j \boldsymbol{v}_j \tag{18}$$

where $\{\xi_j\}_j$ are i.i.d. standard Gaussian. Choose $\boldsymbol{v}_1 = \boldsymbol{u}_{ik}^{*}$ where

$$\boldsymbol{u}_{ik}^{*} = \boldsymbol{z}_{ik}^{*}/||\boldsymbol{z}_{ik}^{*}|| = \boldsymbol{z}_{ik}^{*}/\beta_{ik} \tag{19}$$

is a unit vector in the direction of the design point $\boldsymbol{z}_{ik}^{*}$. The remaining basis vectors $\{\boldsymbol{v}_2, \ldots, \boldsymbol{v}_n\}$ are chosen as an orthonormal basis in the orthogonal complement $V_{ik}^{\perp}$ of the subspace spanned by $\boldsymbol{z}_{ik}^{*}$:

$$V_{ik}^{\perp} = \{\boldsymbol{z} \in \mathbb{R}^n : \langle \boldsymbol{z}, \boldsymbol{z}_{ik}^{*} \rangle = 0\} \tag{20}$$

Consider now the condition of F_{ik}^+ on $\boldsymbol{Z}$ and hence on the random variables $\{\xi_j\}_j$ appearing in (18). Note that

$$Y_i(k) = \frac{\sigma_{ik}^2}{b_i(k)}\langle \boldsymbol{z}_{ik}^*, \boldsymbol{Z}\rangle = \frac{\sigma_{ik}^2}{b_i(k)}\langle \boldsymbol{z}_{ik}^*, \sum_{j=1}^n \xi_j \boldsymbol{v}_j\rangle = \frac{\sigma_{ik}^2}{b_i(k)}\sum_{j=1}^n \xi_j \langle \boldsymbol{z}_{ik}^*, \boldsymbol{v}_j\rangle \tag{21}$$

But $\langle \boldsymbol{z}_{ik}^*, \boldsymbol{v}_1\rangle = \langle \beta_{ik}\boldsymbol{u}_{ik}^*, \boldsymbol{u}_{ik}^*\rangle = \beta_{ik}||\boldsymbol{u}_{ik}^*||^2 = \beta_{ik}$ and $\langle \boldsymbol{z}_{ik}^*, \boldsymbol{v}_j\rangle = 0$ for $j \geq 2$ since $\boldsymbol{v}_j$ $(j \geq 2)$ are orthogonal to $\boldsymbol{v}_1$ and hence $\boldsymbol{z}_{ik}^*$. Consequently, (21) becomes

$$Y_i(k) = \xi_1 \frac{\sigma_{ik}^2}{b_i(k)}\beta_{ik} = \xi_1 \sigma_{ik} \tag{22}$$

The up-crossing failure event is then given by

$$F_{ik}^+ = \{Y_i(k) > b_i(k)\} = \{\xi_1 > b_i(k)/\sigma_{ik}\} = \{\xi_1 > \beta_{ik}\} \tag{23}$$

which imposes conditioning on ξ_1 only. Thus, the conditional vector $\boldsymbol{Z}_{ik}^+$ distributed as $p(\boldsymbol{z}|F_{ik}^+)$ can be simulated as

$$\boldsymbol{Z}_{ik}^+ = \alpha \boldsymbol{u}_{ik}^* + \sum_{j=2}^n \xi_j \boldsymbol{v}_j \tag{24}$$

where α is standard Gaussian conditional on $\{\alpha > \beta_{ik}\}$, that is, $p(\alpha) = \phi(\alpha)U(\alpha - \beta_{ik})/\Phi(-\beta_{ik})$ and $\{\xi_j\}_j$ are i.i.d. standard Gaussian.

The foregoing results are applicable to the down-crossing event F_{ik}^-, except that the design point for F_{ik}^- is the negative of the design point for F_{ik}^+. Also, a random vector $\boldsymbol{Z}_{ik}^-$ distributed as $p(\boldsymbol{z}|F_{ik}^-)$ is identically distributed as $-\boldsymbol{Z}_{ik}^+$.

For the out-crossing event $F_{ik} = F_{ik}^+ \cup F_{ik}^-$, since F_{ik}^+ and F_{ik}^- are disjoint, F_{ik} has two design points corresponding to those from F_{ik}^+ and F_{ik}^-. The probability content of F_{ik} is simply the sum of those of F_{ik}^+ and F_{ik}^-, so $P(F_{ik}) = 2\Phi(-\beta_{ik})$. The input random vector $\boldsymbol{Z}_{ik}$ distributed according to $p(\boldsymbol{z}|F_{ik})$ is distributed as $\boldsymbol{Z}_{ik}^+$ with probability $1/2$ and as $\boldsymbol{Z}_{ik}^-$ with probability $1/2$.

3.2 Interaction of elementary failure regions

The results in the last section indicate that the failure regions corresponding to the elementary failure events can be described in a simple way. Their probabilistic properties are completely determined by their design points, which are known and can be computed

readily from deterministic dynamic analysis. The complexity of the first-excursion problem, however, lies in the interaction of the elementary failure events F_{ik} in forming the first-excursion failure event $F = \cup_{i=1}^{m} \cup_{k=1}^{n_t} F_{ik}$.

Two types of interaction between the elementary failure events can be distinguished. The first one involves interaction of the first-excursion events $\{\cup_{k=1}^{n_t} F_{ik}\}_i$ among the different outputs $i = 1, \ldots, m$. The second type is the interaction of the elementary failure events at different failure time steps k for a given output i. The first type depends on the relationship between the outputs of the system, and would be different for different types of systems and definition of output states. This type of interaction should be studied for a particular type of system, and will not be pursued here. The second type of interaction between the failure events at different failure time steps k, however, can be studied in general, since it depends on the relationship of the response at different instants for a given output, and consequently it is governed by more general properties such as the continuity of the impulse response functions of the system. In this study, we will focus on the second type of interaction. For this purpose, we will examine the simple case of a single-input single-output time-invariant linear system with constant threshold level and excited by stationary white noise, that is, $l = m = 1$ and $b_i(k) = b_1(k) = b$ is constant. The failure event will be $F = \cup_{k=1}^{n_t} F_k$, where $F_k = \{|Y(k)| > b\}$ and we have dropped the index on the output for simplicity in notation.

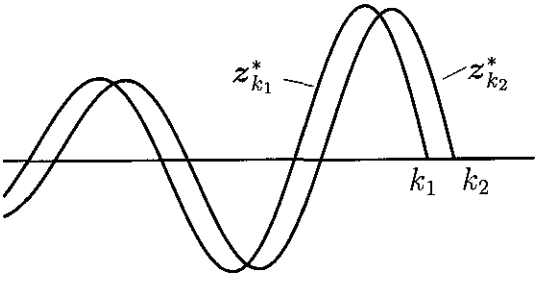

Figure 1: Neighboring design points

SDOF time-invariant linear system

The set of elementary failure events $\{F_k : k = 1, \ldots, n_t\}$ corresponds to the failure of the output response at the consecutive time steps $t_1, \ldots, t_{n_t}$. These elementary failure events evolve approximately in a continuous fashion as k varies. Let $g(k, s) = g(k - s + 1)$ and $h(t, \tau) = h(t - \tau)$ be respectively the impulse response for the discrete- and continuous-time

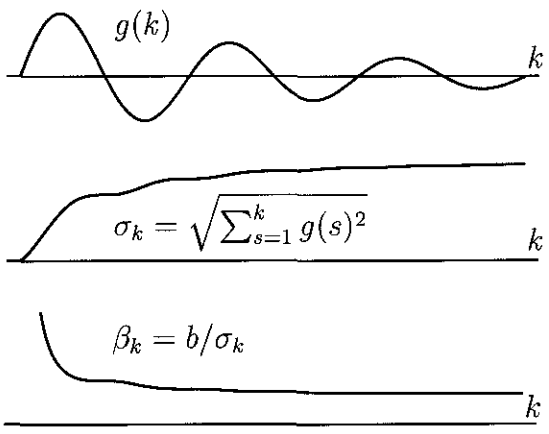

Figure 2: Variation with time of reliability index β_k, response standard deviation σ_k and impulse response $g(k)$

systems. The design point of F_k is then given by $\boldsymbol{z}_k^*(s) = U(k-s)\sqrt{2\pi S\Delta t}\, g(k-s+1)b/\sigma_k^2$. For small Δt, $g(k-s+1) \sim h(t_k - t_s)$, so $\boldsymbol{z}_k^*(s) \sim U(t_k - t_s)\sqrt{2\pi S\Delta t}\, h(t_k - t_s)b/\sigma_k^2$ and correspondingly $w_k^*(t_s) = \sqrt{2\pi S/\Delta t}\, \boldsymbol{z}_k^*(s) \sim 2\pi S\, U(t_k - t_s)h(t_k - t_s)b/\sigma_k^2$, which evolves smoothly with k when h is continuous. This is illustrated in Figure 1, where design points $\boldsymbol{z}_{k_1}^*$ and $\boldsymbol{z}_{k_2}^*$ corresponding to two different failure times k_1 and k_2 are shown. The design points corresponding to two consecutive failure times will be very close, and their distance tends to zero as $\Delta t \to 0$. In fact, Appendix A.2 shows that their distance is $O(\Delta t)$. The distance of the design point from the origin, given by $\beta_k = b/\sigma_k$, decreases gradually with increasing k accordingly as σ_k increases with k, as shown in Figure 2. Due to causality, only the first k components of the design point $\boldsymbol{z}_k^*$ are nonzero, so as k increases by 1, the design point has one more nonzero component in a new dimension. Thus, as k increases, the set of design points $\{\boldsymbol{z}_k^*\}_k$ 'spiral' towards the origin in the n_t-dimensional input variable space which form a continuous path as $\Delta t \to 0$. This path ends when k is largest, that is, $k = n_t$, at the 'global design point' $\boldsymbol{z}^* = \boldsymbol{z}_{n_t}^*$, defined as the design point with the smallest Euclidean norm, or equivalently, reliability index, among all other design points. Note that in the general case of multiple-input multiple-output systems, the failure time of the global design point is not necessarily equal to T, for example, when $b_i(k)$ is not constant or the excitation is modulated by an envelope function.

In the case of a continuous-time single-input-single-output time-invariant system considered for a duration of T, the excitation corresponding to the global design point is a

continuous function of time, given by $w^*(t) = U(T-t)h(T-t)b/\sigma_T^2$, which has been obtained by Drenick as the 'critical excitation' for aseismic design (Drenick 1970). It was noted as the 'smallest energy' (in the sense of Euclidean norm) excitation which pushes the response at time T to the threshold level b. Since $w^*(t)$ is the excitation with the smallest energy which pushes the response at T to the threshold, and it requires more energy to fail at earlier times, it was concluded that if the structure is designed so that it will not fail when the excitation is $w^*(t)$, then it will not fail over time interval $[0, T]$ for any excitation with energy less than that of $w^*(t)$, equal to b/σ_T. Finally, the reader is referred to Appendix A for some additional observations on the failure region for SDOF time-invariant linear systems.

4 Development of importance sampling density

In this section, we develop an efficient ISD based on the knowledge about the failure region F explored in the previous section. For simplicity in notation, we will refer to the design points with a single index as $\{\boldsymbol{z}_i^* : i = 1, \ldots, n_t m\}$ without special regard to the indexes $i = 1, \ldots, m$ and $k = 1, \ldots, n_t$.

The analysis of the failure region F in the last section provides valuable information for constructing an efficient ISD to compute the first-excursion probability. In particular, the elementary failure events are completely characterized by their design point which can be computed readily by deterministic dynamic analysis. It is thus natural to construct the ISD based on the design points to account for the contributions from the elementary failure regions. Since there are $n_t m$ design points, one is concerned with how many and which design points to use. Using more design points may potentially increase the computational effort, and it is often sufficient to use only those that are 'important'. The importance of an elementary failure event F_i may be measured by the conditional probability $P(F_i|F)$, as the latter gives the plausibility that the failure F is due to F_i. Since the ratio of the conditional probabilities of two elementary failure events F_i and F_j is

$$\frac{P(F_i|F)}{P(F_j|F)} = \frac{P(F_i \cap F)/P(F)}{P(F_j \cap F)/P(F)} = \frac{P(F_i)}{P(F_j)} \tag{25}$$

and hence equal to the ratio of their unconditional probabilities, the relative importance of a given design point $\boldsymbol{z}_i^*$ may be quantified based on the (unconditional) probability $P_i = P(F_i) = 2\Phi(-\beta_i)$ of the corresponding elementary failure event F_i. The larger the P_i, the more important the design point $\boldsymbol{z}_i^*$. Since the global design point $\boldsymbol{z}^*$ is by definition the one with the smallest β_i and hence largest P_i, it is natural to center the ISD at it. However, as noted before, the design points that are neighbors of the global design point $\boldsymbol{z}^*$ are very close to $\boldsymbol{z}^*$ (see Figure 1). Their reliability index and hence the probability content of the corresponding elementary failure region are also very close to those of $\boldsymbol{z}^*$. As illustrated in Figure 2, the reliability index drops dramatically for small k and then settles for moderate values of k when the impulse response function $g(k)$ has decayed considerably. So it is only in the case when the duration T is sufficiently small that the global design point assumes significantly more importance than all other design points. In the usual case when the duration T is large compared to the time when the impulse response has decayed sufficiently, the design points in the neighborhood of the global design point are

also important, and should therefore be included to construct the ISD. Since β_k settles quickly with k, the number of design points n_D that should be included is of the order of the total number of time steps, that is, $n_D = O(n_t)$. Thus, as a result of the interaction between the elementary failure events for different failure times, a much larger number of design points in addition to the global design point are important and have to be included in constructing the ISD.

Regarding the choice of the functional form for the ISD, the fundamental criteria are: (1) the value of the ISD can be evaluated readily; and (2) there exists a method to efficiently simulate samples distributed according to the ISD. These criteria are fundamental since the evaluation of the ISD and the simulation of its samples have to be carried out repeatedly during simulation. In constructing an ISD which should account for the contributions from the neighborhood of multiple design points, one important observation is that if one can simulate a sample according to the individual PDF $f_i(\boldsymbol{z})$, which is designed to account for the contribution from the i-th design point, then one can also simulate a sample according to a weighted sum of the f_is, that is, $f(\boldsymbol{z}) = \sum_{i=1}^{n_D} w_i f_i(\boldsymbol{z})$, where $w_i \geq 0$ and $\sum_{i=1}^{n_D} w_i = 1$. This is because a sample distributed as f can be obtained by first drawing random variable I from $\{1, \ldots, n_D\}$ with corresponding probabilities $\{w_1, \ldots, w_{n_D}\}$, and then drawing a sample from $f_I(\boldsymbol{z})$. For this reason, a conventional choice for an ISD using the n_D design points is a weighted sum of Gaussian PDFs among the design points (Schuëller and Stix 1987; Melchers 1989; Au et al. 1999), that is,

$$f(\boldsymbol{z}) = \sum_{i=1}^{n_D} w_i \phi(\boldsymbol{z} - \boldsymbol{z}_i^*) \tag{26}$$

The failure probability will then be estimated by

$$P_F \approx \frac{1}{N} \sum_{r=1}^{N} \frac{\mathbb{I}_F(\boldsymbol{Z}_r') \phi(\boldsymbol{Z}_r')}{\sum_{i=1}^{n_D} w_i \phi(\boldsymbol{Z}_r' - \boldsymbol{z}_i^*)} \tag{27}$$

where $\{\boldsymbol{Z}_r'\}_r$ are i.i.d. samples simulated from f. For application to the first-excursion problem under study, this choice is not efficient, however, since for each sample the evaluation of the quotient $\phi(\boldsymbol{Z}_r') / \sum_{i=1}^{n_D} w_i \phi(\boldsymbol{Z}_r' - \boldsymbol{z}_i^*)$ involves $n_D \times n = O(n_t^2 ml)$ evaluations of the one-dimensional Gaussian PDF. This imposes severe computational burden on the importance sampling procedure since the number of time steps n_t is often large and the number of outputs m may be large even for medium size systems.

4.1 Proposed ISD

The drawback of the ISD in (26) stems from the fact that the variation of the original PDF $\phi(\boldsymbol{z})$ with respect to $\boldsymbol{z}$ is different from that of the individual PDFs $\phi(\boldsymbol{z}-\boldsymbol{z}_i^*)$, otherwise the variation will be canceled out in the importance sampling quotient $\phi(\cdot)/f(\cdot)$. This drawback may be avoided by choosing the ISD as a weighted sum of PDFs which follow the variation of $\phi(\boldsymbol{z})$ and whose samples can be simulated. At this point, it is noted that the conditional PDF of the elementary event F_i, $p(\boldsymbol{z}|F_i) = \phi(\boldsymbol{z})\mathbb{I}_{F_i}(\boldsymbol{z})/P(F_i)$, has this desirable property, since $\mathbb{I}_{F_i}(\boldsymbol{z})$ is constant within F_i. Also, using the representation for the conditional sample in (24), the samples distributed as $p(\boldsymbol{z}|F_i)$ can be simulated. It is thus proposed to construct the ISD as a weighted sum of the conditional PDFs $p(\boldsymbol{z}|F_i) = \phi(\boldsymbol{z})\mathbb{I}_{F_i}(\boldsymbol{z})/P(F_i)$, that is,

$$f(\boldsymbol{z}) = \sum_{i=1}^{n_t m} w_i\, p(\boldsymbol{z}|F_i) = \sum_{i=1}^{n_t m} w_i \frac{\phi(\boldsymbol{z})\mathbb{I}_{F_i}(\boldsymbol{z})}{P(F_i)} \tag{28}$$

where $\{w_i\}_i \geq 0$ and $\sum_{i=1}^{n_t m} w_i = 1$ are the chosen weights associated with the i-th elementary failure event F_i. The weight w_i controls the relative frequency of samples simulated from $p(\boldsymbol{z}|F_i)$, and may be chosen to reflect the relative importance of the elementary failure event in contributing to P_F. In this study, the weights are chosen to be proportional to the probability content of F_i:

$$w_i = \frac{P(F_i)}{\sum_{j=1}^{n_t m} P(F_j)} = \frac{P_i}{\sum_{j=1}^{n_t m} P_j} \tag{29}$$

Substituting (29) into (28), the proposed ISD f is then given by

$$f(\boldsymbol{z}) = \frac{\phi(\boldsymbol{z})}{\sum_{i=1}^{n_t m} P_i} \sum_{i=1}^{n_t m} \mathbb{I}_{F_i}(\boldsymbol{z}) \tag{30}$$

Using f in (30) as the importance sampling density, the first-excursion probability P_F can be expressed as

$$\begin{aligned} P_F &= \int \frac{\phi(\boldsymbol{z})\mathbb{I}_F(\boldsymbol{z})}{f(\boldsymbol{z})} f(\boldsymbol{z})d\boldsymbol{z} \\ &= (\sum_{i=1}^{n_t m} P_i) \int \frac{\mathbb{I}_F(\boldsymbol{z})}{\sum_{i=1}^{n_t m} \mathbb{I}_{F_i}(\boldsymbol{z})} f(\boldsymbol{z})d\boldsymbol{z} \\ &= \hat{P}_F \times \mathsf{E}_f[\frac{1}{\sum_{i=1}^{n_t m} \mathbb{I}_{F_i}(\boldsymbol{Z})}] \end{aligned} \tag{31}$$

where

$$\hat{P}_F = \sum_{i=1}^{n_t m} P_i = 2 \sum_{i=1}^{m} \sum_{k=1}^{n_t} \Phi(-\beta_{ik}) \tag{32}$$

and the subscript f on the expectation in (31) indicates that the expectation is taken with $\boldsymbol{Z}$ distributed according to f instead of ϕ. Also, the fact that $\mathbb{I}_F(\boldsymbol{Z}) = 1$ for every sample $\boldsymbol{Z}$ simulated according to f has been used in the third equality in (31). The first-excursion probability P_F is estimated by simulation as

$$P_F \approx \tilde{P}_F = \hat{P}_F \times \frac{1}{N} \sum_{r=1}^{N} \frac{1}{\sum_{i=1}^{n_t m} \mathbb{I}_{F_i}(\boldsymbol{Z}_r)} \tag{33}$$

where $\{\boldsymbol{Z}_r\}_r$ are i.i.d. samples simulated according to f.

4.2 Simulation of samples according to the proposed ISD

To complete the methodology, the method for efficient simulation of samples distributed as the proposed ISD f given in (30) is presented in this section. Since f is a weighted sum of the conditional PDFs $p(\boldsymbol{z}|F_i)$, its samples can be readily simulated if an efficient method is available for simulating each $p(\boldsymbol{z}|F_i)$, which is discussed next.

The elementary failure event F_i consists of the up-crossing and down-crossing events, F_i^+ and F_i^-, which are mutually exclusive and have the same probability content. As mentioned before, a sample distributed according to $p(\boldsymbol{z}|F_i)$ is distributed as $\boldsymbol{Z}_i^+$ with probability $1/2$ and as $\boldsymbol{Z}_i^-$ with probability $1/2$, where $\boldsymbol{Z}_i^+$ and $\boldsymbol{Z}_i^-$ are distributed as $p(\boldsymbol{z}|F_i^+)$ and $p(\boldsymbol{z}|F_i^-)$, respectively. Since $\boldsymbol{Z}_i^-$ is identically distributed as $-\boldsymbol{Z}_i^+$, the simulation can thus be implemented by simulating $\boldsymbol{Z}_i^+$ only, which is discussed next.

In principle, $\boldsymbol{Z}_i^+$ can be simulated using the representation in (24). To generate a sample using the representation, one has to form the orthonormal basis $\{\boldsymbol{v}_j\}_j$. This may be accomplished, for example, by a Gram-Schmidt orthogonalization procedure. Since n is often large and the orthogonalization has to be done for every different sample during simulation, the orthogonalization procedure could result in significant computational effort. Fortunately, it can be avoided by using an equivalent simulation formula which produces a random vector identically distributed as the component $\sum_{j=2}^{n_t m} \xi_j \boldsymbol{v}_j$ in (24) and is orthogonal to $\boldsymbol{z}_i^*$. In particular, it is observed that when $\boldsymbol{Z}$ is a n-dimensional standard Gaussian vector with independent components, the vector

$$\boldsymbol{Z}_i^{\perp} = \boldsymbol{Z} - \langle \boldsymbol{Z}, \boldsymbol{u}_i^* \rangle \boldsymbol{u}_i^* \tag{34}$$

is orthogonal to $\boldsymbol{u}_i^*$ and has independent Gaussian components with respect to the orthonormal basis $\{\boldsymbol{v}_j : j \geq 2\}$, and hence it is identically distributed as $\sum_{j=2}^{n_t m} \xi_j \boldsymbol{v}_j$. The details of the proof are given in the Appendix. Thus, replacing the sum $\sum_{j=2}^{n_t m} \xi_j \boldsymbol{v}_j$ in (24) by $\boldsymbol{Z}_i^{\perp}$ in (34), the random vector $\boldsymbol{Z}_i^{+}$ distributed according to $p(\cdot|F_i^{+})$ can be simulated as

$$\boldsymbol{Z}_i = \boldsymbol{Z} + (\alpha - \langle \boldsymbol{Z}, \boldsymbol{u}_i^* \rangle)\boldsymbol{u}_i^* \tag{35}$$

where α has a Gaussian distribution conditional on $\alpha > \beta_i$ and $\boldsymbol{Z}$ is a n-dimensional standard Gaussian vector with independent components. Finally, the following representation may be used to simulate α which can be easily derived using an inverse transformation of random variables:

$$\alpha = \Phi^{-1}[U + (1 - U)\Phi(\beta_i)] \tag{36}$$

where U is uniformly distributed on $[0, 1]$.

4.3 Properties of proposed ISD and failure probability estimator

Except for the term involving the sum of indicator functions, the variation of the ISD $f(\boldsymbol{z})$ in (30) follows exactly that of the original density $\phi(\boldsymbol{z})$. Since the weight $w_i = P_i / \sum_{j=1}^{n_t m} P_j$ in (29) associated with the i-th elementary failure region is nonzero if the latter has nonzero probability content P_i, the support region of f, that is, the region in the space of $\boldsymbol{z}$ where $f(\boldsymbol{z}) > 0$, is $\cup_{i=1}^{n_t m} F_i = F$. Thus, all samples simulated according to f will lie in F, while at the same time the whole failure region F is covered by the support region of the ISD and hence the samples generated from it. The latter implies that the contribution from all parts of the failure region will be accounted for in the estimator. Thus, the estimator $\tilde{P}_F$ will be an unbiased estimator of the failure probability P_F. This can be seen directly by taking the expectation of $\tilde{P}_F$ defined in (33) and then using (31) to show that $\mathsf{E}_f[\tilde{P}_F] = P_F$.

The estimator $\tilde{P}_F$ in (33) is a product of $\hat{P}_F$ and the average over N samples of the importance sampling quotient R given by:

$$R(\boldsymbol{Z}) = \frac{1}{\sum_{i=1}^{n_t m} \mathbb{I}_{F_i}(\boldsymbol{Z})} \tag{37}$$

To compute $\tilde{P}_F$, only the average of $R(\boldsymbol{Z})$ needs to be computed by simulation. For each sample, the evaluation of $R(\boldsymbol{Z})$ does not involve the evaluation of probability densities, in

contrast with the case when the ISD in (26) is used, which involves $O(n_t^2 ml)$ computations of Gaussian PDFs. Note that the denominator of R, $\sum_{i=1}^{n_t m} \mathbb{I}_{F_i}(\boldsymbol{Z})$, is just the number of time steps with absolute response lying above the threshold level, and can be obtained easily from the simulated response by a simple counting procedure.

The coefficient of variation (c.o.v.) δ of the failure probability estimator $\tilde{P}_F$, defined as the ratio of the standard deviation to the mean of $\tilde{P}_F$, is given by:

$$\delta = \frac{\sqrt{\mathsf{Var}[\tilde{P}_F]}}{P_F} = \frac{\Delta}{\sqrt{N}} \tag{38}$$

where Δ is the c.o.v. of the importance sampling quotient:

$$\Delta = \frac{1}{P_F}\sqrt{\mathsf{Var}[\frac{\phi(\boldsymbol{Z})\mathbb{I}_F(\boldsymbol{Z})}{f(\boldsymbol{Z})}]} \tag{39}$$

Since $1/n_t m \leq 1/\sum_{i=1}^{n_t m} \mathbb{I}_{F_i} \leq 1$, we see that

$$\frac{\hat{P}_F}{n_t m} \leq \tilde{P}_F \leq \hat{P}_F \tag{40}$$

This result imposes bounds on the random quantity $\tilde{P}_F$, which depends on the simulated samples $\{\boldsymbol{Z}_r\}_r$, and is a stronger result than bounds on the expectation of $\tilde{P}_F$, that is, $\hat{P}_F/n_t m \leq P_F \leq \hat{P}_F$. The bounded property of the estimator $\tilde{P}_F$ is a desirable one, since it implies that $\tilde{P}_F$ will not jump to a significantly large value during simulation. This property is not shared by importance sampling estimators using a conventional choice of ISD, since it is often not possible to put explicit bounds on the importance sampling quotient R. Moreover, by noting that $\sum_{i=1}^{n_t m} \mathbb{I}_{F_i}(\boldsymbol{z}) = n_t m$ when $||\boldsymbol{z}|| \to \infty$, we have

$$\frac{\phi(\boldsymbol{z})}{f(\boldsymbol{z})} = \frac{\sum_{i=1}^{n_t m} P_i}{\sum_{i=1}^{n_t m} \mathbb{I}_{F_i}(\boldsymbol{z})} \to \frac{\hat{P}_F}{n_t m} < \infty \quad \text{as } ||\boldsymbol{z}|| \to \infty \tag{41}$$

This means that the proposed ISD f always has a 'thicker tail' than the original PDF $\phi(\boldsymbol{z})$ of the input random variables, and so contributions from regions at infinity are always accounted for.

When $\{F_i\}_i$ are mutually exclusive, $\mathbb{I}_{F_i}(\boldsymbol{Z}) = 1$ for one and only one i, and $\mathbb{I}_{F_j}(\boldsymbol{Z}) = 0$ for $j \neq i$. This is true for every sample $\boldsymbol{Z}$, and so $1/\sum_{i=1}^{nn_t} \mathbb{I}_{F_i}(\boldsymbol{Z}) \equiv 1$. This means

$$P_F = \tilde{P}_F = \hat{P}_F \tag{42}$$

and hence the ISD f is equal to the optimal ISD when the elementary failure events are mutually exclusive. It can be expected that when the failure events $\{F_i\}_i$ are close to being mutually exclusive, the importance sampling quotient R will be close to unity, which leads to smaller variation in $\tilde{P}_F$ and hence faster convergence to P_F.

Finally, we note that

$$P_F = (\sum_{i=1}^{n_t m} P_i \Delta t) \times \mathsf{E}[\frac{1}{\sum_{i=1}^{n_t m} \mathbb{I}_{F_i}(\boldsymbol{Z})\Delta t}] = (\sum_{i=1}^{n_t m} P_i \Delta t)\mathsf{E}[\frac{1}{T_f}] \tag{43}$$

where $T_f = \sum_{i=1}^{n_t m} \mathbb{I}_{F_i}(\boldsymbol{Z})\Delta t$ is a discrete approximation to the sum of the amount of time that each output response lies above the threshold when $\boldsymbol{Z}$ is distributed as f. On the other hand, let $T_\phi = \sum_{i=1}^{n_t m} \mathbb{I}_{F_i}(\boldsymbol{Z})\Delta t$ be the sum of the amount of time that the absolute response of each output lies above the threshold when $\boldsymbol{Z}$ is distributed as the original PDF ϕ. Then

$$\mathsf{E}[T_\phi] = \mathsf{E}[\sum_{i=1}^{n_t m} \mathbb{I}_{F_i}(\boldsymbol{Z})\Delta t] = \sum_{i=1}^{n_t m} \mathsf{E}[\mathbb{I}_{F_i}(\boldsymbol{Z})]\Delta t = \sum_{i=1}^{n_t m} P_i \Delta t \tag{44}$$

and so

$$P_F = \mathsf{E}[T_\phi] \times \mathsf{E}[\frac{1}{T_f}] \tag{45}$$

which relates the failure probability P_F to the expected times T_f and T_ϕ that the response process spends above the threshold levels.

5 Summary of proposed importance sampling procedure

1. Perform dynamic analysis to obtain impulse response functions $\{g_{ij}(k,s)\}_{ijks}$ which define the input-output relationship of the system. For time-invariant systems, $g_{ij}(k,s) = g_{ij}(k-s+1)$ and only l (the number of inputs) dynamic analyses are required.

2. Compute the output response standard deviations $\{\sigma_{ik}\}_{ik}$ by (11), the elementary reliability indexes $\{\beta_{ik}\}_{ik}$ by (15), the elementary failure probabilities $\{P_{ik}\}_{ik}$ by

$$P_{ik} = 2\Phi(-\beta_{ik}), \tag{46}$$

the upper bound for failure probability by

$$\hat{P}_F = \sum_{i=1}^{m}\sum_{k=1}^{n_t} P_{ik} \tag{47}$$

and the weights $\{w_{ik}\}_{ik}$ by

$$w_{ik} = \frac{P_{ik}}{\sum_{i=1}^{m}\sum_{k=1}^{n_t} P_{ik}} = \frac{P_{ik}}{\hat{P}_F} \tag{48}$$

3. Compute the failure probability estimate $\tilde{P}_F$ by

$$\tilde{P}_F = \hat{P}_F \times \frac{1}{N}\sum_{r=1}^{N} \frac{1}{\sum_{i=1}^{m}\sum_{k=1}^{n_t} \mathbb{I}_{F_{ik}}(\boldsymbol{Z}_r)} \tag{49}$$

where $\{\boldsymbol{Z}_r : r = 1,\ldots,N\}$ are i.i.d. samples generated from the proposed ISD given by

$$f(\boldsymbol{z}) = \frac{\phi(\boldsymbol{z})}{\hat{P}_F}\sum_{i=1}^{m}\sum_{k=1}^{n_t} \mathbb{I}_{F_{ik}}(\boldsymbol{z}) \tag{50}$$

.

To simulate a sample $\boldsymbol{Z}_r$ $(r = 1,\ldots,N)$ according to the proposed ISD given by (50):

(a) Draw a random order pair (I,K) of indexes from the set $\{(i,k)\}_{ik}$ with corresponding probabilities $\{w_{ik}\}_{ik}$.

(b) Simulate $\boldsymbol{Z}$ as a n-dimensional standard Gaussian vector with independent components; U_1 and U_2 as uniform variables on $[0,1]$. Compute

$$\alpha = \Phi^{-1}[U_1 + (1 - U_1)\Phi(\beta_{IK})] \tag{51}$$

and set

$$\boldsymbol{Z}_r = \begin{cases} \boldsymbol{Z} + (\alpha - \langle \boldsymbol{Z}, \boldsymbol{u}^*_{IK} \rangle)\boldsymbol{u}^*_{IK} & \text{if } U_2 \leq 1/2 \\ -\boldsymbol{Z} - (\alpha - \langle \boldsymbol{Z}, \boldsymbol{u}^*_{IK} \rangle)\boldsymbol{u}^*_{IK} & \text{otherwise} \end{cases} \tag{52}$$

where $\boldsymbol{u}^*_{IK} = \boldsymbol{z}^*_{IK}/\beta_{IK}$ and $\boldsymbol{z}^*_{IK}$ is defined by (10).

Equations (48), (49), (51) and (52) are analogous to (29), (33) and (36) and (35), respectively, except the indexes on output i and time step k are now written explicitly for clarity.

It is worth-noting that once the unit impulse response functions are computed in Step 1, the response of the structure can be computed by convoluting them with the excitation to evaluate each $\mathbb{I}_{F_{ik}}(\boldsymbol{Z}_r)$ $(r = 1, \ldots, N)$. This can be done efficiently using the FFT algorithm and its inverse. This approach may save computational effort, since the setup of structural matrices in the finite element model, for example, can be avoided in the repeated computations of structural response for different excitations during simulation.

6 Numerical applications

6.1 Example 1: SDOF oscillator

Consider a single-degree-of-freedom (SDOF) oscillator with natural frequency frequency $\omega = 2\pi$ rad/s (i.e., 1 Hz) and damping ratio $\zeta = 2\%$ subjected to white noise excitation:

$$\ddot{Y}(t) + 2\zeta\omega\dot{Y}(t) + \omega^2 Y(t) = W(t) \tag{53}$$

where $W(t)$ is a Gaussian white noise process with spectral intensity $S = 1$. The sampling interval is assumed to be $\Delta t = 0.05$ s and the duration of study is $T = 15$ s. The total number of time points, and hence the number of input random variables is thus $n_t = T/\Delta t + 1 = 15/0.05 + 1 = 301$. Failure is defined as the absolute displacement response exceeding a threshold level b, that is, $F = \cup_{k=1}^{n_t}\{|Y(t_k)| > b\}$ where $t_k = (k-1)\Delta t$, $k = 1, \ldots, n_t$. The impulse response function $h(t)$ of the system is given by

$$h(t) = \frac{e^{-\zeta\omega t}}{w_d} \sin \omega_d \, t \tag{54}$$

where $w_d = w\sqrt{1-\zeta^2}$ is the damped natural frequency. Figure 3 shows the variation of $h(t)$ within the duration of study. The variance of $y(t)$ is given by integrating the square of $h(\tau)$ up to time t:

$$\sigma^2(t) = \int_0^t h(\tau)^2 \, d\tau \tag{55}$$

The standard deviation $\sigma(t)$ is shown in Figure 4. Note that $\sigma(t)$ is increasing with t and its wavy character is due to the oscillatory behavior of the impulse response function $h(t)$.

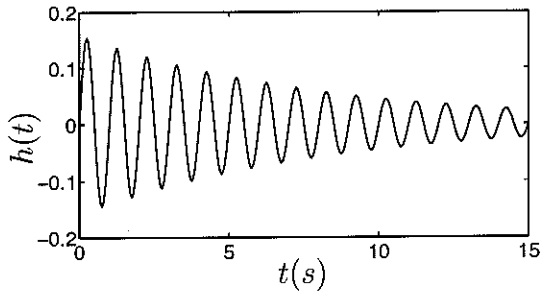

Figure 3: Impulse response function $h(t)$

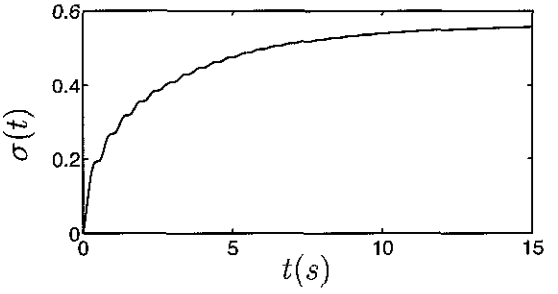

Figure 4: Standard deviation of response, $\sigma(t)$

The first-excursion probability P_F for a given threshold level b is computed by importance sampling using the following three choices of ISD: (1) ISD centered at the global design point with unit covariance matrix; (2) ISD centered among all the n_t design points with unit covariance matrix, as given in (26); (3) the proposed ISD in (50). The weights used in (26) for Choice (2) are given by (48). Figure 5 shows the variation of the weights with time t for $b = 3, 4, 5 \times \sigma(T)$, where $\sigma(T)$ is the standard deviation of the response at time $T = 15$ s, being the largest within the duration of study. Note that, although Figures 3-5 plot the quantities $h(t)$, $\sigma(t)$ and $w(t)$ as a continuous function of time t, only the values at the discrete time instants $t_k = (k-1)\Delta t$, $k = 1, \ldots, n_t$, are evaluated and used in the actual computations.

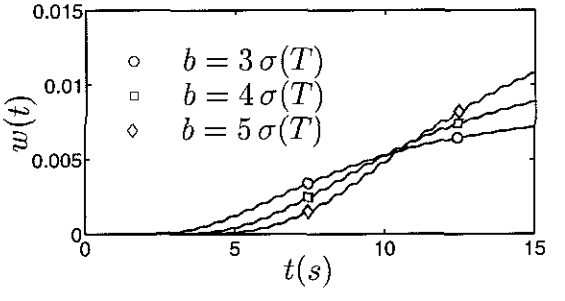

Figure 5: Weight $w(t)$

The failure probability estimates for the three threshold levels are shown in Figure 6 for different sample sizes N. The results computed with ISD using Choices (1), (2) and (3) are shown with dotted, dashed and solid lines, respectively. For comparison, the results computed by standard Monte Carlo simulation (MCS) with 10^6 samples are shown as

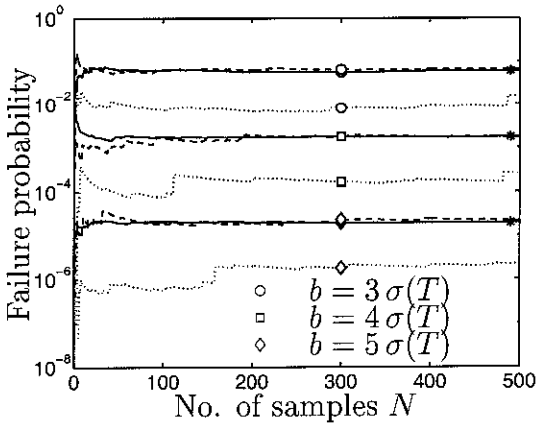

Figure 6: Failure probability estimates for different threshold levels b and number of samples N. Choice (1): dotted lines; Choice (2): dashed lines; Choice (3): solid lines; MCS with 10^6 samples: asterisks

asterisks in the figure.

From Figure 6, it can be seen that results computed by Choice (1) are practically biased within the number of samples considered, showing that it is not suitable for computing the first-excursion probability. In particular, the failure probability estimates corresponding to Choice (1) are smaller than the exact failure probabilities by orders of magnitude. Note that this is not due to most of the samples generated by the ISD of Choice (1) lying in the safe region. In fact, the percentages of the 500 samples generated by the ISD of Choice (1) that lie in the failure region are 63%, 57% and 53%, showing that more than half of the samples lie in the failure region. Rather, the practical bias observed in Choice (1) is due to the fact that the importance sampling quotient in Choice (1) takes on values which are orders of magnitude smaller than the probability of failure for most of the generated samples. The sudden 'jumps' in the simulation history of failure probability estimates of Choice (1) correspond to those rare occasions where the importance sampling quotient is much larger than the rest of the samples.

The results computed using Choices (2) and (3) have similar variability, although the latter has even smaller variability. The results for both Choices (2) and (3) converge to the target failure probability when N increases. To assess quantitatively the variability of the estimates and hence the efficiency of the importance sampling procedure using the different choices, the c.o.v. (coefficient of variation) of the importance sampling quotients

Table 1: The c.o.v. Δ of importance sampling quotients for failure probability

$b/\sigma(T)$	P_F	Δ			
		Choice (1)	Choice (2)	Choice (3) (Proposed)	MCS
3	6.01×10^{-2}	28.9	1.80	1.24	3.95
4	1.79×10^{-3}	63.1	3.19	0.93	23.6
5	1.97×10^{-5}	69.3	4.36	0.80	226

defined by (39) for the three choices are estimated from the 500 simulated samples. Note that the c.o.v. δ of the failure probability estimate using N samples is given by (38). For Choice (1), the values of Δ are estimated using 100,000 samples, since the estimates for failure probability and hence c.o.v. using 500 samples are biased. The results are shown in Table 1. Using the c.o.v. for the importance sampling quotient, the number of samples N_δ required to achieve a c.o.v. of δ in the failure probability estimate, given by $N = \Delta^2/\delta^2$ is also computed. For the results shown in Table 2, $\delta = 30\%$ has been used, which represents a moderate level of accuracy in the failure probability estimate.

Table 1 shows that the c.o.v.s Δ for Choice (1) are much larger than those of Choices (2) and (3). Also, for higher values of P_F, even standard MCS is more efficient than using Choice (1). The corresponding number of samples N_δ in Table 2 for Choice (1) are larger by orders of magnitude than those for Choices (2) and (3). The c.o.v.s for Choice (3) are smaller than those for Choice (2). The number of samples for Choice (3) required to achieve a c.o.v. of $\delta = 30\%$ is remarkably small (< 20) compared with those commonly reported in the importance sampling literature, implying that the proposed ISD leads to a very efficient importance sampling strategy. This superior efficiency is made possible through the use of analytical results on the first-excursion problem specifically for linear systems.

6.2 Example 2: Seismic response of moment-resisting steel frame

Consider a six-story moment-resisting steel frame as shown in Figure 7 with member sections given in Table 3. For each floor, the same section is used for all girders. The structure

Table 2: Number of samples N_δ to achieve a c.o.v. of $\delta = 30\%$ in $\tilde{P}_F$

$b/\sigma(T)$	P_F	N_δ ($\delta = 30\%$)			
		Choice (1)	Choice (2)	Choice (3) (Proposed)	MCS
3	6.01×10^{-2}	9302	37	18	174
4	1.79×10^{-3}	44,233	114	10	6206
5	1.97×10^{-5}	53,400	212	8	565,558

is modeled as a two-dimensional linear frame with beam elements connecting the joints of the frame. Masses are lumped at the nodes of the frame, which include the contributions from the dead load of the floors and the frame members. They are tabulated in Table 4. The natural frequencies of the first two modes are computed to be 0.552 Hz and 1.56 Hz, respectively. Rayleigh damping is assumed so that the first two modes have 5% of critical damping.

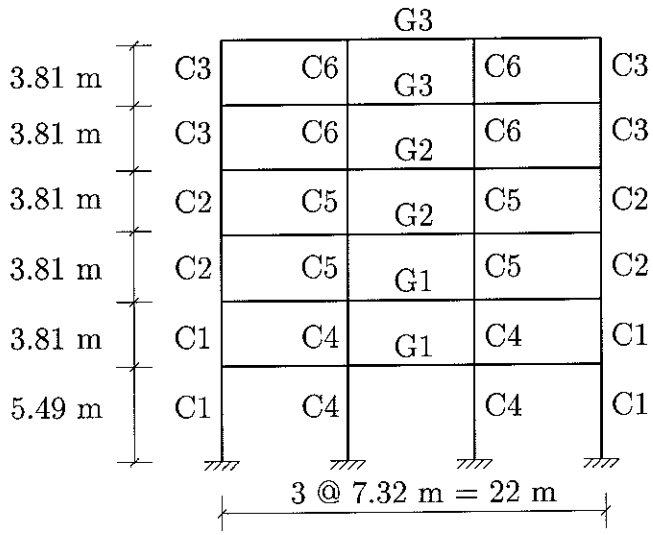

Figure 7: Moment-resisting frame structure

The structure is subjected to a stochastic ground acceleration $\ddot{a}(t)$ modeled by filtered

Table 3: Sections (AISC) for frame members

Story	Exterior Column	Interior Column	Girder
1, 2	C1: W14 × 159	C4: W27 × 161	G1: W24 × 94
3, 4	C2: W14 × 132	C5: W27 × 114	G2: W24 × 76
5, 6	C3: W14 × 99	C6: W24 × 84	G3: W24 × 55

Table 4: Point Masses

Floor	Exterior Column ($\times 10^3$ kg)	Interior Column ($\times 10^3$ kg)
2	60.4	81.0
3	53.3	78.1
4	51.9	76.0
5	51.7	75.8
6	50.1	73.5
Roof	44.6	63.1

white noise with a Clough-Penzien spectrum and modulated by an envelope function $e(t)$:

$$\ddot{a}(t) + 2\zeta_{s2}\omega_{s2}\dot{a}(t) + \omega_{s2}^2 a(t) = 2\zeta_{s1}\omega_{s1}\dot{a}_1(t) + \omega_{s1}^2 a_1(t) \tag{56}$$

$$\ddot{a}_1(t) + 2\zeta_{s1}\omega_{s1}\dot{a}_1(t) + \omega_{s1}^2 a_1(t) = e(t)W(t) \tag{57}$$

where $\omega_{s1} = 15.7$ rad/s (2.5 Hz) and $\omega_{s2} = 1.57$ rad/s (0.25 Hz) are the dominant and lower-cutoff frequency of the spectrum; $\zeta_{s1} = 0.6$ and $\zeta_{s2} = 0.8$ are the damping parameters associated with the dominant and lower-cutoff frequency, respectively. The envelope function $e(t)$ is assumed to vary quadratically as $(t/4)^2$ for the first 4 seconds, then settle at unity for 10 seconds, and finally decay as $\exp[-(t-14)^2/2]$ starting from $t = 14$ s. In (57), $W(t)$ is the Gaussian white noise with spectral intensity $S = 1 \times 10^{-3} m^2/s^3$.

The input-output relationship between the input $W(t)$ and the output $Y_i(t)$ is

$$Y_i(t) = \int_0^t h_i(t-\tau)e(\tau)W(\tau)d\tau \tag{58}$$

where $h_i(\tau)$ is the impulse response of the augmented system which include the dynamics of the frame structure and the soil layers represented by the Clough-Penzien spectrum. The variance of $Y_i(t)$ is given by

$$\sigma_i^2(t) = 2\pi S \int_0^t h_i(t-\tau)^2 e(\tau)^2 d\tau \tag{59}$$

Note that both the response $Y_i(t)$ and its variance $\sigma_i^2(t)$ can be obtained by convolution. A duration of $T = 30$ s and a time interval of $\Delta t = 0.02$ s are used in computing the response of the structure, leading to $n_t = T/\Delta t + 1 = 30/0.02 + 1 = 1501$ input random variables in the discrete approximation for $W(t)$.

Peak Interstory drift ratio

Consider the failure probability that the peak interstory drift ratio over all stories of the structure exceeds a threshold level b. The outputs $\{Y_i : i = 1, \ldots, m\}$ consist of the interstory drift ratio of all columns connecting two consecutive floors. There are thus $m = 24$ outputs, which can be expressed as a linear transformation of the state variables of the structure. The impulse response for the interstory drift ratios of the exterior columns at every floor are shown in the first column of Figure 8. These are obtained from one dynamic analysis of the structure. Although not shown in the figure, it is noted that the impulse response for the interior columns are close to those for the corresponding exterior columns.

The standard deviations $\sigma_i(t)$ $(i = 1, \ldots, 6)$ computed based on (59) by numerical convolution are shown in the second column in Figure 8. The elementary failure probability for the i-th interstory drift ratio, $P_i(t) = P(|y_i(t)| > b) = 2\Phi(-b/\sigma_i(t))$, are also computed with $b = 1\%$ and shown in the third column in Figure 8. Although the quantities in Figure 8 are shown as a continuous function of t, only the values at the discrete time instants $t_k = (k-1)\Delta t$, $k = 1, \ldots, n_t$, are evaluated in the actual computations. It is seen in Figure 8 that the variation of the response standard deviation $\sigma_i(t)$ with t follows approximately that of the envelope function $e(t)$. In particular, the maximum standard deviation for each response over the duration of study occurs at $t = 14$ s, which coincides with the time when the envelope function starts to decay. The variation of the elementary failure probabilities with time is sharper than that of the corresponding response standard deviations. According to (44), the area under the curve of each $P_i(t)$ gives the expected time that the absolute response for the i-th story spends above the threshold level. The ratio of the area under the elementary failure probability $P_i(t)$ between different stories

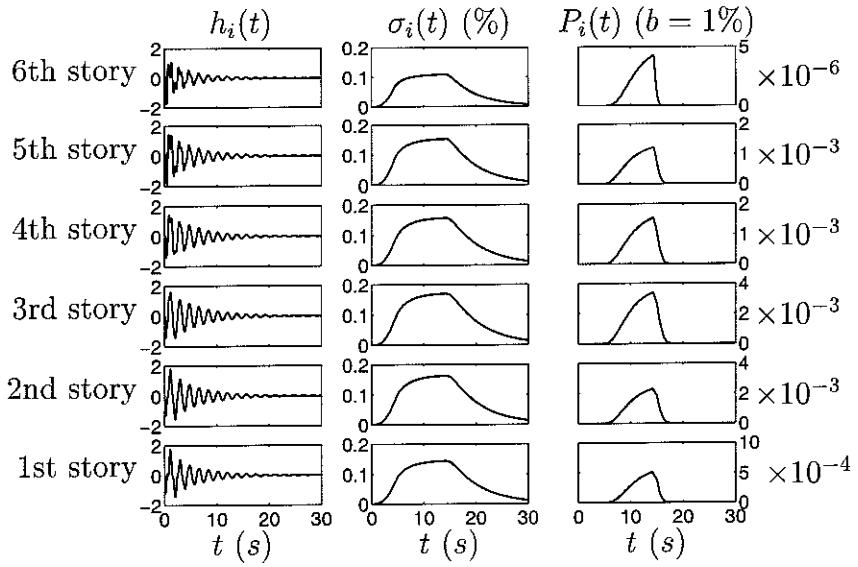

Figure 8: Impulse response $h_i(t)$, standard deviation $\sigma_i(t)$ and elementary failure probability $P_i(t)$ for interstory drift ratios

i gives an idea of the relative importance of the responses in contributing to the first-excursion failure. Thus, from Figure 8, it can be expected the second to fifth story should give the main contribution to the failure probability.

The failure probability estimates $\tilde{P}_F$ for the threshold levels $b = 0.5\%, 0.75\%$ and 1% are shown in Figure 9 for different number of samples N. The estimates by standard Monte Carlo simulation with $10,000$ samples are also computed and shown with circles in the figure. Note that the Monte Carlo estimate for $b = 1\%$ is not shown in the figure, since the sample size is not large enough to provide a sufficiently accurate estimate for the failure probability corresponding to this threshold level. From Figure 9, it can be seen that the failure probability estimates computed using the proposed ISD converge quickly to the target probability of failure.

To investigate quantitatively the variability of the failure probability estimates, the c.o.v. Δ of the importance sampling quotient is computed using 200 samples and shown in Table 5. The number of samples required to achieve a c.o.v. of $\delta = 30\%$ in the failure probability estimate are shown in the last column of the table. In general, the c.o.v. Δ for the importance sampling quotient is quite small, and consequently only a small number of samples N_δ is required to achieve a c.o.v. of $\delta = 30\%$ in the failure probability estimates. The values of N_δ show that a sufficiently good failure probability estimate can be obtained

Table 5: The c.o.v. Δ of proposed importance sampling quotient for failure probability for peak interstory drift ratio

b (%)	$\tilde{P}_F$ $(N = 200)$	Δ	N_δ $(\delta = 30\%)$
0.5	6.41×10^{-2}	1.34	20
0.75	2.79×10^{-4}	1.15	15
1	1.23×10^{-7}	1.09	13

Table 6: Failure probability estimates for peak interstory drift ratio with $N = 20$ samples

b (%)	$\tilde{P}_F$ $(N = 200)$	Run	$\tilde{P}_F$ $(N = 20)$
0.5	6.41×10^{-2}	1	4.54×10^{-2}
		2	4.29×10^{-2}
		3	7.28×10^{-2}
0.75	2.79×10^{-4}	1	1.77×10^{-4}
		2	3.14×10^{-4}
		3	2.55×10^{-4}
1	1.23×10^{-7}	1	1.21×10^{-7}
		2	1.43×10^{-7}
		3	1.22×10^{-7}

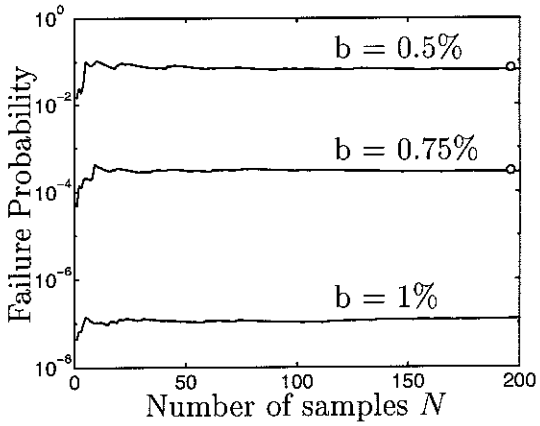

Figure 9: Failure probability estimates for peak interstory drift ratio for different threshold levels b and number of samples N. MCS estimates with $10,000$ samples are shown with circles

with a small sample size of, say, $N = 20$. To demonstrate this, independent simulation runs are carried out with $N = 20$ samples to compute the failure probability estimates. The results are shown in Table 6, which demonstrate that the variability of the failure probability estimates among independent runs is indeed small.

Peak floor acceleration

Finally, consider the failure probability that the (absolute horizontal) peak floor acceleration over all stories of the structure exceeds (in magnitude) a threshold level b (in %g). As the horizontal displacement along the beam elements for the girders are linearly interpolated, this probability is equal to the failure probability that the horizontal absolute acceleration at any one of the nodes of the frame exceeds the threshold level b. There are thus $m = 24$ outputs, corresponding to the absolute horizontal acceleration at the 24 nodes of the frame. The results are shown in Figures 10, 11, Tables 7 and 8, in analogy with the results for the peak interstory drift in Figures 8, 9, Tables 5 and 6, respectively. Similar to the case of peak interstory drifts, these results show that fast convergence is achieved in the failure probability estimates. In particular, Table 7 shows that less than 20 samples are needed to achieve a c.o.v. of $\delta = 30\%$ in all the failure probability estimates, which is verified in Table 8.

Table 7: The c.o.v. Δ of proposed importance sampling quotient for failure probability for peak floor acceleration

b (g)	$\tilde{P}_F$	Δ	N_δ ($\delta = 30\%$)
0.2	3.87×10^{-2}	1.05	12
0.3	2.24×10^{-5}	0.70	5
0.4	6.36×10^{-10}	0.83	8

Table 8: Failure probability estimates for peak floor acceleration with $N = 20$ samples

b (g)	P_F ($N = 200$)	Run	$\tilde{P}_F$ ($N = 20$)
0.2	3.87×10^{-2}	1	2.31×10^{-2}
		2	4.34×10^{-2}
		3	3.10×10^{-2}
0.3	2.24×10^{-5}	1	2.43×10^{-5}
		2	2.76×10^{-5}
		3	3.04×10^{-5}
0.4	6.36×10^{-10}	1	6.34×10^{-10}
		2	5.22×10^{-10}
		3	5.48×10^{-10}

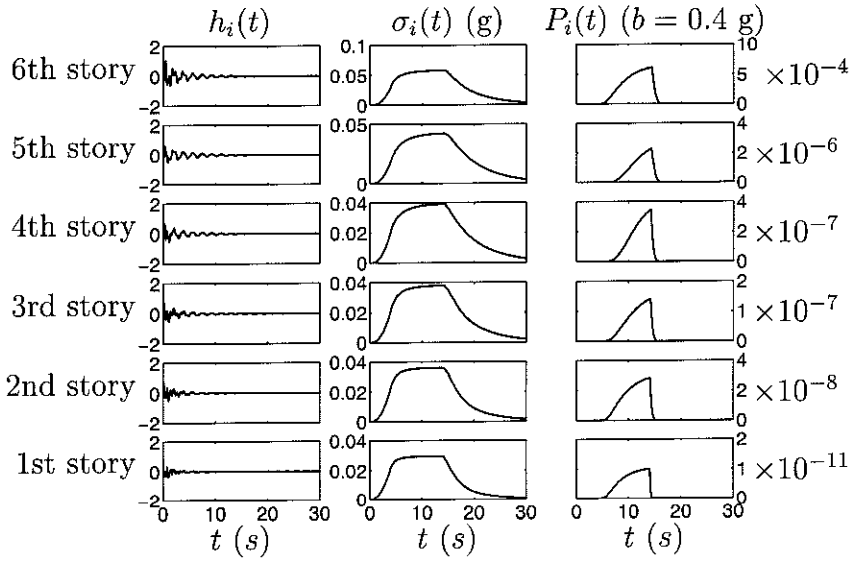

Figure 10: Impulse response $h_i(t)$, standard deviation $\sigma_i(t)$ and elementary failure probability $P_i(t)$ for floor accelerations

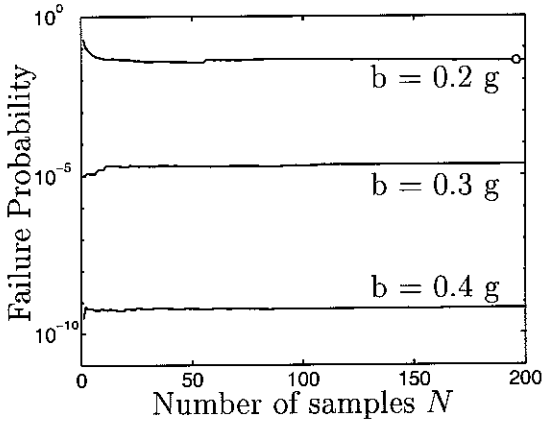

Figure 11: Failure probability estimates for peak floor acceleration for different threshold levels b and number of samples N. MCS estimates with $10,000$ samples are shown with circles

7 Conclusions

The complexity of the first-excursion problem stems from the structure of the union of the elementary failure regions in the high-dimensional excitation space, although these regions are simple to describe. One important consequence of such union structure is that, in addition to the global design point, a large number of neighboring design points are important in accounting for the failure probability, and hence have to be considered in constructing an ISD (importance sampling density). A new ISD is proposed which takes into account the contributions of all the elementary failure regions. It is built upon the following three important observations:

1. Appreciation of the fact that, for time linear invariant systems, the design points corresponding to failure at different time steps can be obtained simply from the unit impulse response function.

2. Appreciation of the fact that, instead of only the global design point, a large number of design points are important in contributing to the failure probability.

3. The novel concept of constructing the ISD as a weighted sum of conditional PDFs rather than just Gaussian PDFs centered at the design points (as is commonly done) so that the original PDF is cancelled out in the importance sampling quotient, therefore making the method extremely efficient, regardless of the size of the problem in terms of the number of time steps, the number of inputs and the number of outputs.

Whereas conventional choices for constructing the ISD using the design points are found to be inefficient, numerical examples show that the proposed ISD leads to very fast convergence in the first-excursion failure probability estimates. Examples have shown that no more than 20 samples are required to achieve a c.o.v. of 30% in the failure probability estimates over a range of five orders of magnitude in the failure probabilities. Furthermore, the required number of samples actually decreases with decreasing failure probability. This efficiency is remarkable, and is unprecedented in the literature to the best of the authors' knowledge. It is achieved because vital information on the first-excursion problem that is gained from an analytical study of the failure region for linear systems is utilized in constructing the proposed ISD.

A Some additional observations on the failure region of SDOF time-invariant linear systems

In this appendix, we present some additional observations on the failure region of SDOF time-invariant linear systems subjected to filtered white noise excitation. The conclusions are expected to hold, however, in more general situations, such as for MDOF systems or filtered white noise excitation, since the essential property underlying these characteristics is the continuity of the unit impulse response function of the system. The discussion is based on continuous-time systems, for the sake of mathematical convenience in analysis, but analogous results hold for discrete-time systems.

We will denote the excitation on the interval $[0,T]$ by $w(t)$, which is assumed to be square-integrable on $[0,T]$, that is, $w \in L^2[0,T]$. The system response corresponding to the excitation w will be denoted by $y(t;w)$:

$$y(t;w) = \int_0^t h(t-\tau)w(\tau)d\tau \tag{60}$$

where h is the unit impulse response function. The failure region will then be $F = \{w \in L^2[0,T] : |y(t;w)| > b \text{ for some } t \in [0,T]\}$.

A.1 Neighborhood of points in the failure region

Proposition: Except for points on the failure boundary, every point w in the failure region has a neighborhood of radius $\rho(w)$ lying entirely inside the failure region where

$$\rho(w) = \sup_{\tau \in [0,T]} \frac{|y(\tau;w)| - b}{||h||_\tau} \tag{61}$$

and

$$||h||_\tau = \sqrt{\int_0^\tau h(s)^2 ds} \tag{62}$$

is the Euclidean norm of the unit impulse function h on the interval $[0,\tau]$. In other words, if w is an interior point of F, then $w + \Delta w$ is also an interior point of F for all $\Delta w(t)$ with $||\Delta w||_T < \rho(w)$.

Proof: Let w be an interior point of F. Then $\exists\, \tau \in [0,T]$ such that $|y(\tau;w)| - b > 0$. At such τ, for any Δw with $||\Delta w||_T < [|y(\tau;w)| - b]/||h||_\tau$,

$$\begin{aligned}
|y(\tau;\Delta w)| &\leq \int_0^\tau |h(\tau - s)\Delta w(s)|ds \\
&\leq \sqrt{\int_0^\tau h(\tau-s)^2 ds}\sqrt{\int_0^\tau \Delta w(s)^2 ds} \\
&= ||h||_\tau ||\Delta w||_\tau \\
&\leq ||h||_\tau ||\Delta w||_T \\
&< ||h||_\tau \frac{|y(\tau;w)| - b}{||h||_\tau} \\
&= |y(\tau;w)| - b
\end{aligned} \tag{63}$$

That is,

$$|y(\tau;w)| - |y(\tau;\Delta w)| > b \tag{64}$$

Now,

$$\begin{aligned}
|y(\tau; w + \Delta w)| &= |y(\tau;w) + y(\tau;\Delta w)| \quad \text{by linearity} \\
&\geq |y(\tau;w)| - |y(\tau;\Delta w)| > b
\end{aligned} \tag{65}$$

and so $w + \Delta w$ is an interior point of F. In general, choosing τ from $\mathbb{T}(w) = \{\tau \in [0,T] : |y(\tau;w)| > b\}$ to maximize $[|y(\tau;w)| - b]/||h||_\tau$, we conclude for any Δw:

$$||\Delta w||_T < \sup_{\tau \in \mathbb{T}(w)} \frac{|y(\tau;w)| - b}{||h||_\tau} \quad \Rightarrow \quad w + \Delta w \text{ is an interior point of } F \tag{66}$$

Finally, since for all $s \in \{[0,T] - \mathbb{T}(w)\}$, $[|y(s;w)| - b]/||h||_s \leq 0 < \sup_{\tau \in \mathbb{T}(w)}[|y(\tau;w)| - b]/||h||_\tau$, the value of the supremum in (66) is unaffected by taking over all $\tau \in [0,T]$. We thus have

$$||\Delta w||_T < \rho(w) = \sup_{\tau \in [0,T]} \frac{|y(\tau;w)| - b}{||h||_\tau} \quad \Rightarrow \quad w + \Delta w \text{ is an interior point of } F \tag{67}$$

and hence the proof.

A.2 Proximity of neighboring design points

Proposition: The (Euclidean) distance between neighboring design points corresponding to consecutive up-crossing (down-crossing) failure times separated by sufficiently small Δt is $O(\Delta t)$.

Proof: Let $\{w_t^*(\tau) : \tau \in [0,T]\}$ be the design point corresponding to the elementary up-crossing failure event at time t: $F_t^+ = \{y(t) > b\}$. We start by studying the difference $w_{t+\Delta t}^*(\tau) - w_t^*(\tau)$ on $[0,T]$. First note that $w_t^*(\tau) \equiv 0$ for $\tau > t$ and $w_{t+\Delta t}^*(\tau) \equiv 0$ for $\tau > t + \Delta t$. Thus, for $\tau \in (t + \Delta t, T]$,

$$w_{t+\Delta t}^*(\tau) - w_t^*(\tau) \equiv 0 \tag{68}$$

and for $\tau \in (t, t + \Delta t)$,

$$w_{t+\Delta t}^*(\tau) - w_t^*(\tau) = w_{t+\Delta t}^*(\tau) \tag{69}$$

For $\tau \in (0,t)$, we approximate $w_{t+\Delta t}^*(\tau) - w_t^*(\tau)$ with a first order Taylor expansion with respect to t for small Δt:

$$w_{t+\Delta t}^*(\tau) - w_t^*(\tau) \sim \frac{\partial w_t^*(\tau)}{\partial t}\,\Delta t \tag{70}$$

Since $\tau \in (0,t)$, $w_t^*(\tau)$ is given by:

$$w_t^*(\tau) = h(t-\tau)\frac{b}{||h||_t^2} \tag{71}$$

which gives, upon partial differentiation with respect to t,

$$\frac{\partial w_t^*(\tau)}{\partial t} = b\left[\frac{h'(t-\tau)}{||h||_t^2} - \frac{h(t-\tau)h(t)^2}{||h||_t^4}\right] \tag{72}$$

Thus, the square of the Euclidean distance between $w_{t+\Delta t}^*$ and w_t^* is given by:

$$\begin{aligned} ||w_{t+\Delta t}^* - w_t^*||_T^2 &= \int_0^T |w_{t+\Delta t}^*(\tau) - w_t^*(\tau)|^2\, d\tau \\ &= \int_0^{t+\Delta t} |w_{t+\Delta t}^*(\tau) - w_t^*(\tau)|^2 d\tau \quad \text{by (68)} \\ &= \int_0^t |w_{t+\Delta t}^*(\tau) - w_t^*(\tau)|^2\, d\tau + \int_t^{t+\Delta t} |w_{t+\Delta t}^*(\tau)|^2\, d\tau \quad \text{by (69)} \end{aligned} \tag{73}$$

Using (70), the first term on the R.H.S. of (73) is approximated by:

$$\int_0^t |w_{t+\Delta t}^*(\tau) - w_t^*(\tau)|^2 d\tau \sim \int_0^t \left(\frac{\partial w_t^*(\tau)}{\partial t}\Delta t\right)^2 d\tau = O(\Delta t^2) \tag{74}$$

On the other hand, the second term on the R.H.S. of (73) is approximated by:

$$\int_t^{t+\Delta t} |w_{t+\Delta t}^*(\tau)|^2\, d\tau \sim w_{t+\Delta t}^*(t)^2 \Delta t = \frac{h(t+\Delta t - t)^2}{||h||_{t+\Delta t}^4}\, b^2\, \Delta t = O(\Delta t^3) \tag{75}$$

since $h(\Delta t)^2 = O(\Delta t^2)$. So, using (73), (74) and (75), to the leading order of Δt^2,

$$||w^*_{t+\Delta t} - w^*_t||^2_T \sim \int_0^t \left(\frac{\partial w^*_t(\tau)}{\partial t}\right)^2 d\tau\, \Delta t^2 \tag{76}$$

Now for $\tau \in (0, t)$, using (72),

$$\left(\frac{\partial w^*_t(\tau)}{\partial t}\right)^2 = b^2 \left[\frac{h'(t-\tau)^2}{||h||^4_t} - 2\frac{h'(t-\tau)h(t-\tau)h(t)^2}{||h||^6_t} + \frac{h(t-\tau)^2 h(t)^4}{||h||^8_t}\right] \tag{77}$$

Integrating (77) with respect to τ from 0 to t, and noting that

$$\int_0^t h'(t-\tau)^2 d\tau = ||h'||^2_t \tag{78}$$

$$\int_0^t h'(t-\tau)h(t-\tau)d\tau = \frac{1}{2}h(t)^2 \tag{79}$$

$$\int_0^t h(t-\tau)^2\, d\tau = ||h||^2_t \tag{80}$$

we have

$$\int_0^t \left(\frac{\partial w^*_t(\tau)}{\partial t}\right)^2 d\tau = b^2\, \frac{||h'||^2_t}{||h||^4_t} \tag{81}$$

Finally, using (76) and (81), we have:

$$||w^*_{t+\Delta t} - w^*_t||_T \sim b\Delta t \frac{||h'||_t}{||h||^2_t} = O(\Delta t) \tag{82}$$

and hence the proof.

A.3 Overshooting of design point response

Proposition: For continuous time systems, the response corresponding to the design point at up-crossing (down-crossing) failure time t will over-shoot the level b after time t. However, the duration of overshoot (over which the response has exceeded the level b) is $O(h(t)^2/||h'||^2_t)$ and the maximum amount of overshoot is $O(h(t)^4/||h||^2_t||h'||^2_t)$, and are thus very small for stable systems at sufficiently large t.

This proposition is somewhat counter-intuitive. One may expect from intuition that the maximum value of the response $y(\tau; w^*_t)$ corresponding to the excitation w^*_t occurs

at time t, since w_t^* is by definition the excitation with the smallest 'energy' that drives the response to the level b at time t and so should not 'waste' any additional amount of energy to drive the response above b. The proposition says that such a 'waste' of energy is unavoidable, although the amount is very small in common situations when the failure time t is sufficiently large that the unit impulse response has decayed sufficiently compared to $||h||_t$ or $||h'||_t$. Indeed, for discrete-time systems, overshooting may not be apparent, due to discretization error and the fact that the overshoot duration is so small that may not be captured with available sampling interval used in numerical integration.

Proof: We first obtain a second order Taylor expansion for the response $y(\tau; w_t^*)$ near time t. For $s > 0$,

$$\begin{aligned} y(t+s; w_t^*) &= \int_0^{t+s} h(t+s-\tau)\frac{h(t-\tau)}{||h||_t^2}U(t-\tau)\, b\, d\tau \\ &= \frac{b}{||h||_t^2}\int_0^t h(t-\tau+s)h(t-\tau)d\tau \quad \text{since } U(t-\tau) \equiv 0 \text{ for } \tau > t \\ &= \frac{b}{||h||_t^2}\int_0^t h(\tau+s)h(\tau)\, d\tau \end{aligned} \tag{83}$$

When s is small,

$$h(\tau+s) \sim h(\tau) + h'(\tau)\, s + \frac{1}{2}h''(\tau)\, s^2 \tag{84}$$

Substituting (84) into (83), integrating and simplifying, we have

$$y(t+s; w_t^*) \sim b + \frac{b\, h(t)^2}{2||h||_t^2}\, s + \frac{b}{2||h||_t^2}\left[h'(t)h(t) - ||h'||_t^2\right]\, s^2 \tag{85}$$

Since the first order term with respect to s is always positive, we see that there is always overshooting. However, the time derivative of the response when it crosses b could be very small for stable systems at large failure time t, since then either $h(t) \to 0$ as $t \to \infty$ for strongly stable systems, or $h(t) < \infty$, $||h||_t \to \infty$ as $t \to \infty$ for marginally stable systems.

The duration of overshoot is equal to the time $\hat{t}$ after t when the response crosses the level b again (and goes below b afterwards). It is approximated by solving $y(t+s; w_t^*) = b$ for s, which yields:

$$\hat{t} = \frac{h(t)^2}{||h'||_t^2 - h'(t)h(t)} \sim \frac{h(t)^2}{||h'||_t^2} \quad \text{for large } t \tag{86}$$

since $h'(t)h(t)$ is small compared to $||h'||_t^2$ for stable systems at large t.

With the quadratic approximation of $y(t+s;w_t^*)$ in (85) for small $s>0$, the time $\hat{s}$ after t at which the overshoot is maximum is simply given by

$$\hat{s} = \frac{\hat{t}}{2} \tag{87}$$

Finally, the maximum amount of overshoot $\delta_{\max}$ is approximated using (85) with $s=\hat{s}$ in (87):

$$\begin{aligned}\delta_{\max} &= y(t+\hat{s};w_t^*) - b \\ &= \frac{b\,h(t)^4}{8||h||_t^2}\left[||h'||_t^2 - h'(t)h(t)\right]^{-1} \\ &\sim \frac{b\,h(t)^4}{8||h||_t^2||h'||_t^2} = O(\frac{h(t)^4}{||h||_t^2||h'||_t^2}) \quad \text{for large } t\end{aligned} \tag{88}$$

A.4 A reciprocal relationship of design point responses

The following proposition holds for time-variant systems as well.

Proposition: For all $s,t \geq 0$,

$$\sigma_s^2 y(t;w_s^*) = \sigma_t^2 y(s;w_t^*) \tag{89}$$

where $\sigma_t^2 = 2\pi S||h||_t^2$ is the response variance at time t.

Proof: Result is trivial when $t=s$. Consider $t>s$,

$$\begin{aligned}\sigma_s^2 y(t;w_s^*) &= \sigma_s^2 \int_0^t h(t,\tau)w_s^*(\tau)d\tau \\ &= 2\pi S \int_0^t h(t,\tau)h(s,\tau)U(s-\tau)d\tau \\ &= 2\pi S \int_0^s h(t,\tau)h(s,\tau)d\tau\end{aligned} \tag{90}$$

since $h(s,\tau) \equiv 0$ for $s<\tau<t$. On the other hand, when $t<s$,

$$\sigma_s^2 y(t;w_s^*) = 2\pi S \int_0^t h(t,\tau)h(s,\tau)d\tau \tag{91}$$

Equations (90) and (91) imply, for all $s,t \geq 0$,

$$\sigma_s^2 y(t;w_s^*) = 2\pi S \int_0^{\min(t,s)} h(t,\tau)h(s,\tau)d\tau \tag{92}$$

The proof then follows from the symmetry of the above expression with respect to s and t.

B Simulation formula for $Z_i^{\perp}$

We show here that the random vector $\boldsymbol{Z}_i^{\perp}$ given by (34) is orthogonal to the unit vector $\boldsymbol{u}_i^*$ and has independent Gaussian components with respect to the basis in the orthogonal complement of $\boldsymbol{u}_i^*$.

Since $\boldsymbol{Z}_i^{\perp}$ given by (34) is a Normal vector, it is sufficient to prove that (1) $\boldsymbol{Z}_i^{\perp}$ is orthogonal to $\boldsymbol{z}_i^*$ and (2) it has uncorrelated components in the $(n-1)$-dimensional orthogonal complement $V_i^{\perp}$ of the one-dimensional subspace spanned by $\boldsymbol{u}_i^*$.

First,

$$\langle \boldsymbol{Z}_i^{\perp}, \boldsymbol{u}_i^* \rangle = \langle \boldsymbol{Z} - \langle \boldsymbol{Z}, \boldsymbol{u}_i^* \rangle \boldsymbol{u}_i^*, \boldsymbol{u}_i^* \rangle = \langle \boldsymbol{Z}, \boldsymbol{u}_i^* \rangle - \langle \boldsymbol{Z}, \boldsymbol{u}_i^* \rangle \langle \boldsymbol{u}_i^*, \boldsymbol{u}_i^* \rangle = 0 \tag{93}$$

since $\langle \boldsymbol{u}_i^*, \boldsymbol{u}_i^* \rangle = ||\boldsymbol{u}_i^*||^2 = 1$.

To show the second claim, first note that $\boldsymbol{Z}_i^{\perp}$ has zero mean, since $\boldsymbol{Z}$ does: $\mathsf{E}[\boldsymbol{Z}_i^{\perp}] = \mathsf{E}[\boldsymbol{Z}] - \langle \mathsf{E}[\boldsymbol{Z}], \boldsymbol{u}_i^*, \boldsymbol{u} \rangle_i^* = \boldsymbol{0}$. By the first claim, $\boldsymbol{Z}_i^{\perp}$ is orthogonal to $\boldsymbol{u}_i^*$ and hence lies in $V_i^{\perp}$, so it has the following Fourier series representation:

$$\boldsymbol{Z}_i^{\perp} = \boldsymbol{Z} - \langle \boldsymbol{Z}, \boldsymbol{u}_i^* \rangle \boldsymbol{u}_i^* = \sum_{j=1}^{n-1} A_j \boldsymbol{v}_j \tag{94}$$

where $\{\boldsymbol{v}_j : j = 1, \ldots, n-1\}$ is an orthonormal basis in $V_i^{\perp}$ and $\{A_j\}_j$ are the Fourier coefficients given by

$$A_j = \langle \boldsymbol{Z}_i^{\perp}, \boldsymbol{v}_j \rangle = \langle \boldsymbol{Z}, \boldsymbol{v}_j \rangle - \langle \boldsymbol{Z}, \boldsymbol{u}_i^* \rangle \langle \boldsymbol{u}_i^*, \boldsymbol{v}_j \rangle = \langle \boldsymbol{Z}, \boldsymbol{v}_j \rangle \tag{95}$$

since $\langle \boldsymbol{u}_i^*, \boldsymbol{v}_j \rangle = 0$ for $\boldsymbol{v}_j \in V_i^{\perp}$. It remains to show that the coefficients $\{A_j\}_j$ are uncorrelated. For $j, k = 1, \ldots, n-1$,

$$\begin{aligned}
\mathsf{E}[A_j A_k] &= \mathsf{E}[\langle \boldsymbol{v}_j, \boldsymbol{Z} \rangle \langle \boldsymbol{Z}, \boldsymbol{v}_k \rangle] \\
&= \mathsf{E}[\boldsymbol{v}_j^T \boldsymbol{Z} \boldsymbol{Z}^T \boldsymbol{v}_k] \\
&= \boldsymbol{v}_j^T \mathsf{E}[\boldsymbol{Z} \boldsymbol{Z}^T] \boldsymbol{v}_k \\
&= \boldsymbol{v}_j^T \boldsymbol{v}_k \quad \text{since } \mathsf{E}[\boldsymbol{Z} \boldsymbol{Z}^T] = \text{Identity matrix} \\
&= \delta_{jk}
\end{aligned} \tag{96}$$

where δ_{jk} is the Kronecker delta: $\delta_{jk} = 1$ if $j = k$ and $\delta_{jk} = 0$ otherwise. Thus $\{A_j\}_j$ are uncorrelated, and the proof is completed.

References

Ang, G. L., A. H.-S. Ang, and W. H. Tang (1992). Optimal importance sampling density estimator. *Journal of Engineering Mechanics, ASCE 118*(6), 1146–1163.

Au, S. K. and J. L. Beck (1999). A new adaptive importance sampling scheme. *Structural Safety 21*, 135–158.

Au, S. K. and J. L. Beck (2000a). Calculation of first excursion probabilities by subset simulation. In *Proceedings of Joint Specialty Conference on Probabilistic Mechanics and Structural Reliability*, Notre Dame, Indiana.

Au, S. K. and J. L. Beck (2000b). Subset simulation: A new approach to calculating small failure probabilities. In *Proceedings of International Conference on Monte Carlo Simulation*, Monte Carlo, Monaco.

Au, S. K., C. Papadimitroiu, and J. L. Beck (1999). Reliability of uncertain dynamical systems with multiple design points. *Structural Safety 21*, 113–133.

Bayer, V. and C. G. Bucher (1999). Importance sampling for first passage problems of nonlinear structures. *Probabilistic Engineering Mechanics 14*, 27–32.

Bergman, L. A. and J. C. Heinrich (1981). Petrov-Galerkin finite element solution for the first passage probability and moments of first passage time of the randomly accelerated free particle. *Computer Methods in Applied Mechanics and Engineering 27*, 345–362.

Bucher, C. G. (1988). Adaptive sampling – an iterative fast Monte Carlo procedure. *Structural Safety 5*, 119–126.

Crandall, S. H., K. L. Chandirmani, and R. G. Cook (1966). Some first passsage problems in random vibration. *Journal of Applied Mechanics, ASME 33*, 624–639.

Der Kiureghian, A. (2000). The geometry of random vibrations and solutions by FORM and SORM. *Probabilistic Engineering Mechanics 15*, 81–90.

Der Kiureghian, A. and T. Dakessian (1998). Multiple design points in first and second-order reliability. *Structural Safety 20*, 37–49.

Dokainish, M. A. and K. Subbaraj (1989). A survey of direct time-integration methods in computational structural dynamics – I. explicit methods. *Computers and Structures 32*(6), 1371–1386.

Drenick, R. F. (1970). Model-free design of aseismic structures. *Journal of Engineering Mechanics, ASCE 96*, 483–493.

Hammersley, J. M. and D. C. Handscomb (1964). *Monte-Carlo Methods.* London: Methuen.

Hughes, T. (1987). *The finite element method: linear static and dynamic finite element analysis.* Prentice-Hall, Inc.

Karamchandani, A., P. Bjerager, and C. A. Cornell (1989). Adaptive importance sampling. In *Proc. 5th ICOSSAR*, San Francisco, pp. 855–862.

Langley, R. S. (1988). A 1st passage approximation for normal stationary random processes. *Journal of Sound and Vibration 122*(2), 261–275.

Lin, Y. K. (1967). *Probabilistic Theory of Structural Dynamics.* McGraw Hill.

Lin, Y. K. and G. Q. Cai (1995). *Probabilistic Structural Dynamics: Advanced Theory and Applications.* New York: McGraw-Hill Book Company.

Lutes, D. L. and S. Sarkani (1997). *Stochastic Analysis of Structural and Mechanical Vibrations.* New Jersey: Prentice Hall.

Mason, A. B. and W. D. Iwan (1983). An approach to the 1st passage problem in random vibration. *Journal of Applied Mechanics, ASME 50*, 641–646.

Melchers, R. E. (1989). Importance sampling in structural systems. *Structural Safety 6*, 3–10.

Naess, A. (1990). Approximate first-passage and extremes of narrow-band Gaussian and non-Gaussian random vibrations. *Journal of Sound and Vibration 138*(3), 365–380.

Papadimitriou, C., J. L. Beck, and L. S. Katafygiotis (1997). Asymptotic expansions for reliabilities and moments of uncertain dynamic systems. *Journal of Engineering Mechanics, ASCE 123*(12), 1219–1229.

Pradlwarter, H. J. and G. I. Schuëller (1997a). Exceedance probability of MDOF-systems under stochastic excitation. *Applied Mechanics Review, ASME 50*(11), 168–173.

Pradlwarter, H. J. and G. I. Schuëller (1997b). On advanced Monte Carlo simulation procedures in stochastic structural dynamics. *International Journal of Non-linear Mechanics 32*(4), 735–744.

Pradlwarter, H. J. and G. I. Schuëller (1999). Assessment of low probability events of dynamical systems by controlled Monte Carlo simulation. *Probabilistic Engineering Mechanics 14*, 213–227.

Pradlwarter, H. J., G. I. Schuëller, and P. G. Melnik-Melnikov (1994). Reliability of MDOF-systems. *Probabilistic Engineering Mechanics 9*, 235–243.

Rice, O. C. (1944). Mathematical analysis of random noise. *Bell System Technical Journal 23*, 282–332.

Rice, O. C. (1945). Mathematical analysis of random noise. *Bell System Technical Journal 24*, 46–156.

Roberts, J. B. (1976). First passage probability for nonlinear oscillators. *Journal of Engineering Mechanics, ASCE 102*, 851–866.

Rubinstein, R. Y. (1981). *Simulation and the Monte-Carlo Method.* New York, N.Y.: John Wiley & Sons, Inc.

Schuëller, G. I., H. J. Pradlwarter, and M. D. Pandey (1993). Methods for reliability assessment of nonlinear systems under stochastic dynamic loading – a review. In *Proceedings of EURODYN'93*, pp. 751–759. Balkema.

Schuëller, G. I. and R. Stix (1987). A critical appraisal of methods to determine failure probabilities. *Structural Safety 4*, 293–309.

Shinozuka, M. (1987). Stochastic fields and their digital simulation. In G. Schuëller and M. Shinozuka (Eds.), *Stochastic Methods in Structural Dynamics*, pp. 93–133. Dordrecht: M. Nijhoff Publishers.

Shinozuka, M. and G. Deodatis (1988). Stochastic process models for earthquake ground motion. *Probabilistic Engineering Mechanics 3*, 114–123.

Soong, T. T. and M. Grigoriu (1993). *Random Vibration of Mechanical and Structural Systems.* Prentice Hall, Inc.

Spencer, B. F. and L. A. Bergman (1993). On the numerical solution of the Fokker-Planck equation for nonlinear stochastic systems. *Nonlinear Dynamics 4*, 357–372.

Subbaraj, K. and M. A. Dokainish (1989). A survey of direct time-integration methods in computational structural dynamics – II. implicit methods. *Computers and Structures 32*(6), 1387–1401.

Vanmarcke, E. H. (1975). On the distribution of the first-passage time for normal stationary random processes. *Journal of Applied Mechanics, ASME 42*, 215–220.

Yang, J. N. and M. Shinozuka (1971). On the first excursion probability in stationary narrow-band random vibration. *Journal of Applied Mechanics, ASME 38*, 1017–1022.